NASA Contractor Report 195394

Ultra-High Bypass Ratio Jet Noise

John K.C. Low
United Technologies Corporation
Pratt & Whitney Division
East Hartford, Connecticut

October 1994

Prepared for
Lewis Research Center
Under Contract NAS3–26618

National Aeronautics and
Space Administration

FOREWORD

This report was prepared under NASA Contract NAS–26618, Task Order No. 6, for NASA Lewis Research Center. The NASA technical monitor was Eugene A. Krejsa. Pratt and Whitney's Task Manager was Douglas C. Mathews.

The author would like to acknowledge the assistances of Richard Czapiga of Pratt and Whitney, John TeVelde and Bob Morton of the United Technologies Research Center in conducting the model jet noise tests.

TABLE OF CONTENTS

1.0 SUMMARY

A 1/15 scale model of the Pratt and Whitney's Advanced Ducted Propulsor (ADP) engine coaxial nozzle was designed by Pratt and Whitney, and built by MicroCraft Incorporated. The model nozzle was tested in the United Technologies Research Center anechoic acoustic research tunnel (ART) over a range of jet noise parameters that matched exactly the jet noise flow conditions of the ADP engine nozzle at seven (7) engine power settings. Jet noise data were acquired at static condition and at wind tunnel Mach numbers of 0.2, 0.27 and 0.35 to simulate inflight effects on jet noise. For the model coaxial nozzle, the secondary nozzle area varied due to varying temperature differences between the primary and secondary streams. The range of secondary to primary nozzle area ratios tested varied from 7.1 to 7.4, with bypass ratios corresponding to 10.2 to 11.8, respectively. This ultra–high bypass ratio (UHBR) jet noise database is over and beyond the limits of today's jet noise prediction databases which are limited to bypass ratio of 6.5 and secondary to primary nozzle area ratio of 3.5.

Results showed that the jet noise from the 1/15 scaled ADP model nozzle can be successfully scaled to the ADP fullscale engine jet noise levels. The predicted levels of jet noise for the ADP engine were significantly lower than the levels predicted for fan and core noise. Fan and core noise dominated the ADP engine noise spectra at most angles for all power settings. Jet noise is shown to dominate only the low frequency portion of the spectra and at the most aft angles (greater than 140 degrees) and only at high ADP engine power setting. For the ADP engine, the major sources in ascending order of importance are jet, core and fan noise.

Comparisons of the UHBR jet noise data with the current Society of Automotive (SAE) Jet Noise Prediction Methods showed that the current prediction methods overpredicted the ADP jet noise by as much as 6 decibels. This is to be expected because jet noise from the UHBR nozzle falls outside today's jet noise database and to predict this UHBR jet noise requires significant extrapolation beyond the current available data. The result suggested that a simple method of subtracting 6 decibels from the SAE Coaxial Jet Noise Prediction may be the most expedient method of predicting the UHBR jet noise for the ADP type coaxial nozzle, until a new coaxial jet noise prediction method can be developed using additional information from this UHBR jet noise database.

The simulated jet noise flight effects with wind tunnel Mach numbers up to 0.35 produced jet noise inflight noise reductions up to 12 decibels. The reductions in jet noise levels were across the entire jet noise spectra, suggesting that the inflight effects affected all source noise components of the coaxial jet, unlike the inflight effects for "mixer type" nozzles where only the low frequency portions of the static jet noise spectra are affected. The relative velocity exponents for the UHBR jet noise flight effects ranged from 5.17 for 90 degrees to 9.58 for 150 degrees directivity angle. This set of values, which is higher than that for the lower bypass ratio turbofan coaxial jets, is the only set of relative velocity exponents for UHBR jet noise available in today's jet

jet noise database. For a given primary jet and flight velocity, the jet noise reduction is predicted to be larger for the UHBR jet than for the lower bypass ratio turbofan jet.

2.0 INTRODUCTION

2.1 BACKGROUND

The next generation of low–noise turbofan engines that will power the Advanced Subsonic Transport (AST) aircraft may be required to meet more stringent noise rules than the current Federal Aviation Regulation (FAR) Part 36 Stage 3. These new low–noise engines will have ultra–high bypass ratios (UHBR) that are almost twice those of the current turbofans, and fan tipspeeds that are significantly lower than any turbofan engine in production today. The Pratt and Whitney's candidate for these next generation low–noise engines is the Advanced Ducted Propulsor (ADP) which has a bypass ratio of 11 to 12 and a fan tipspeed less than 1000 ft/sec at full thrust. Advances in fan technology and the use of the geared low–speed fan in new engines such as the ADP are expected to lower the fan noise source levels to those of the jet and core noise floor. An accurate assessment of these jet and core noise levels is critical to both the cycle selection for the UHBR ADP engines and the establishment of realistic noise goals for the AST aircraft.

Jet noise predictions are generally based on correlations of data from fullscale engines and subscale model exhaust nozzles. Today's jet noise technology database for predicting noise of two–stream coaxial nozzles – such as those envisioned for the UHBR engines – is limited to turbofan engines with bypass ratio up to 6.5 and secondary–to–primary nozzle area ratio up to 3.5. By contrast, the ADP engine exhaust nozzle system has a bypass ratio of 11 to 12 and a nozzle area ratio of 7 to 8. Jet noise from the UHBR exhaust nozzle system thus falls outside today's jet noise database and to predict this jet noise level requires significant extrapolation beyond the current available data.

Jet and core noise spectral characteristics are very similiar and it is difficult to discriminate these noise components from the total noise spectra of the fullscale engine. One procedure that has been used successfully to separate these two noise components is to acquire noise data for both the fullscale engine and a subscale model of only the exhaust nozzle of the engine. The model jet noise data, when scaled to fullscale, is then used to define the jet noise level for the engine, and the core noise level is obtained by taking the total (jet plus core) and subtracting the jet noise from it.

The effects of forward flight are known to be different for jet and for core noise. For today's lower bypass ratio engines, the jet noise flight effect has been measured in various acoustic wind tunnel and flyover experiments. The reduction of jet noise in flight is generally associated with the reduction of the jet's mean shear relative to the surrounding ambient air. For the UHBR engine exhaust nozzle, the cycle is different and the jet velocities for both the primary and the secondary are significantly lower. Thus for a given forward flight speed, the effect of relative jet velocity to forward speed is predicted to be larger for a UHBR engine as compared to today's

turbofan engine. It is not evident that the same relative velocity exponents for turbofan jets would apply to the UHBR jet. The effect of forward flight on the UHBR jet noise must be independently established if static UHBR engine data are to be used to predict aircraft flyover noise levels. Subscale model UHBR jet noise testing in an anechoic wind tunnel is needed to obtain both static and flight jet noise data for the next generation low–noise UHBR engines.

2.2 PROGRAM DESCRIPTION

The major objectives of this program were (1) to develop a static and flight jet noise prediction capability for the ultra–high bypass ratio (UHBR) ADP engines and (2) to assess the relative importances of both jet and core noise in these UHBR engines. Under the program, Pratt and Whitney designed a 1/15 scale model of the ADP demonstrator engine exhaust nozzle which was then built by MicroCraft Incorporated. The nozzle was tested in the United Technologies Research Center (UTRC) anechoic free jet/acoustic research tunnel (ART). The test matrix for the jet noise tests was selected to match exactly the jet noise flow conditions of the ADP exhaust nozzle at seven engine power settings (30 %, 40%, 45%, 79%, 89%, 92% and 100% thrust). Jet noise data were acquired at static condition and at tunnel Mach numbers of 0.2, 0.27 and 0.35. Background wind tunnel noise data were taken for each of the Mach number conditions tested. In the jet noise data reduction, these wind tunnel background noise were subtracted from the measured data. The model jet noise data were then corrected for shear–layer effects and atmospheric absorption and scaled to fullscale for comparison with ADP engine data. Data analyses were focussed on (1) correlation with ADP engine test data and assessment of the relative importances of jet and core noise, (2) comparison of the UHBR model jet noise results with today's jet noise prediction methods derived from lower bypass ratio exhaust nozzles, and (3) correlations of the UHBR jet noise flight effects.

3.0 TEST APPARATUS

The experimental apparatus used in this program is described in this section. Included are descriptions of the 1/15 scale model UHBR exhaust nozzles, the UTRC anechoic freejet/acoustic research tunnel (ART), model nozzles test setup, acoustic measurements setup, instrumentations for controlling and setting jet noise flow parameters and recording performance and acoustic data, and procedure for measuring nozzles axial thermal growths and secondary nozzle area under the elevated jet temperature operating conditions during the tests.

3.1 1/15 SCALE UHBR MODEL NOZZLES

Figure 1 shows a schematic of the 1/15 scale model of the UHBR ADP demonstrator engine exhaust nozzle. The primary nozzle has an area of 3.75 sq.inch under ambient condition. The nozzles are made of 416 Stainless Steel with thermal expansion coefficients of 0.0000096 in/in deg.F. The primary nozzle area changes less than 0.5 percent between the lowest and highest jet temperature condition. The secondary nozzle area, defined by the miminum annulus area bounded by the inner diameter (7.03 inch) of the secondary nozzle exit and the outer diameter of the primary nozzle (shown in Figure 1) is more sensitive to the relative difference in thermal growths between the primary (hot) and the secondary (warm) flow path that includes pipings upstream of the nozzles. The measurement of the actual secondary nozzle area at each test point is described in a later section.

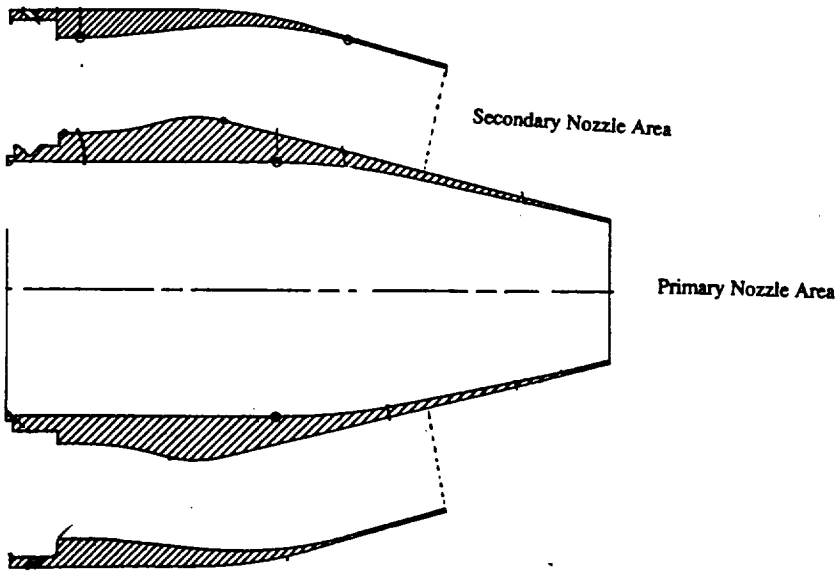

Figure 1. Schematic of the 1/15–Scale UHBR Model Nozzles.

3.2 UTRC ACOUSTIC RESEARCH TUNNEL (ART)

Figure 2 shows a schematic of the UTRC Acoustic Research Tunnel (ART) where the UHBR jet noise tests were conducted. A 36–inch diameter nozzle was used to provide a freestream open jet tunnel flow capable of simulating forward Mach number up to 0.35.

Tunnel Mach number is determined by measuring the pressure ratio (P_{t0}/P_{s0}) in the open jet and calculated based on the isentropic flow conditions as follows:

$$\frac{P_{t0}}{P_{s0}} = \frac{(P_a - dP)}{P_a - delP}$$

where Pa is the barometric pressure, delP is the difference between the tunnel inlet total (Pa) and the chamber static (Pso) and dP is the pressure loss across the inlet screens. The tunnel Mach number, Mo is given by the equation

$$M_0 = \sqrt{\frac{2}{\gamma - 1}\left[\left(\frac{P_{t0}}{P_{s0}}\right)^{\frac{\gamma-1}{\gamma}} - 1\right]}$$

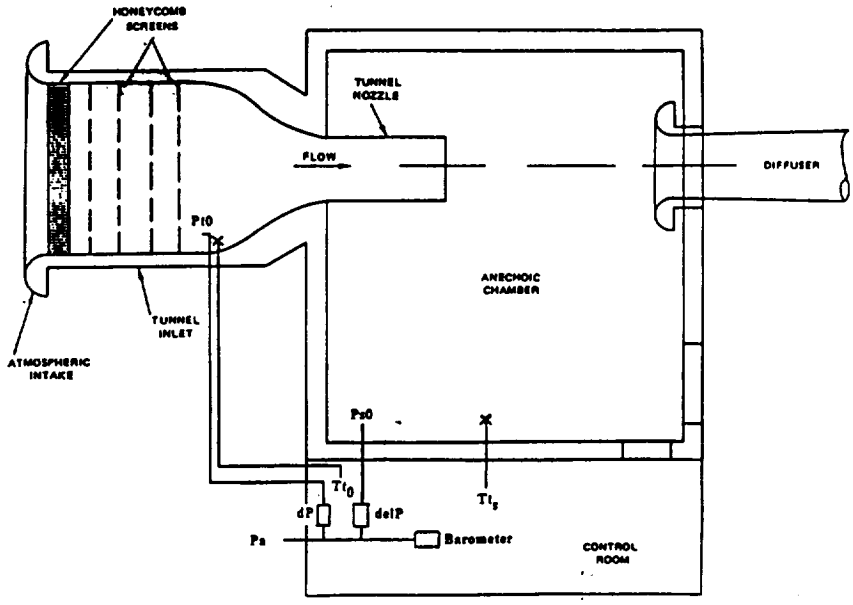

Figure 2. UTRC's ART Tunnel Schematic.

The nozzle flows (primary and secondary) are provided via a coaxial air supply system. A schematic of the supply system is shown in Figure 3.

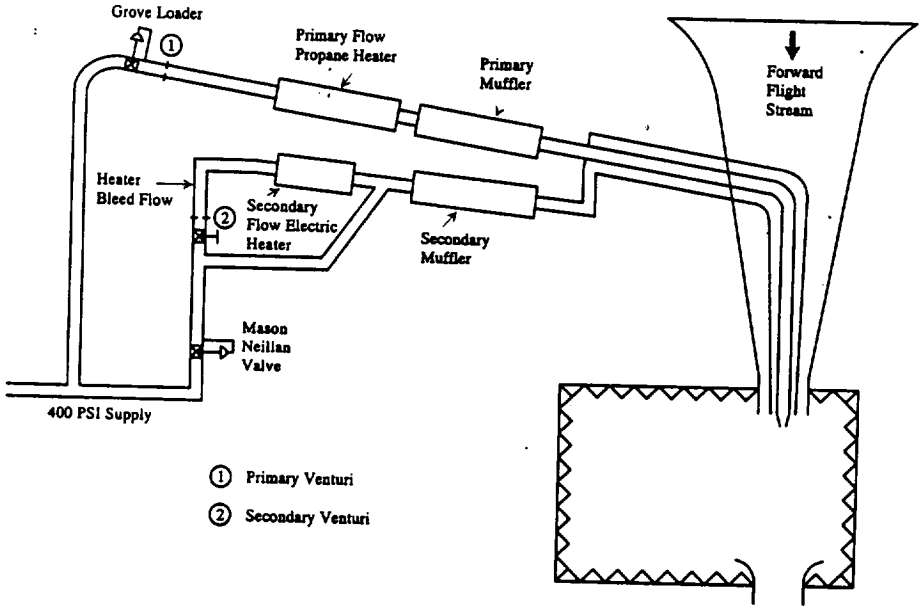

Figure 3. Schematics of the UTRC's ART Primary and Secondary Air Supply System.

The primary core flow is heated by a propane burner which is capable of providing burner exit temperature of 1380 degrees Fahrenheit (F) at line pressure lower than 85 psig. The air supply to the burner is controlled by a Grove regulator and metered by a choked ASME venturi. The propane supply to the burner is shown in Figure 4.

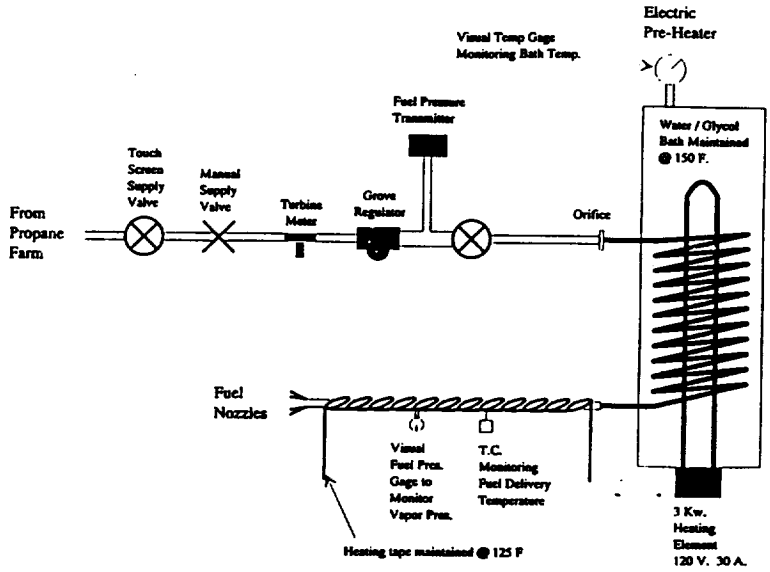

Figure 4. Schematic of the Propane Fuel Supply System to Burner for Heating Primary Air.

The propane is heated downstream of the metering orifice to prevent the propane from re–liquifying in the cold winter weather. This is accomplished by running the propane supply line through a water/glycol hot bath maintained at 175 deg. F. (The heat loss in the propane supply line was quite significant in the winter weather and additional heating tape wrapped around the line downstream of the hot bath and the burner fuel nozzles was required to prevent the propane from re–liquifying.) During burner shakedown, steady combustion and heating of the primary flow was achieved with flow rates as low as 0.2 lb/sec. The heated primary core flow is then fed through a muffler to reduce upstream combustion generated noise and exiting as the primary nozzle air supply.

The secondary flow is also metered by a chocked ASME orifice whose supply pressure is controlled by a throttling Mason–Neillan valve. An electric heater is used to heat the secondary air to the desired temperature. However, because the heater is designed for low flows (typically less than 1.25 lb/sec.) only a portion of the total secondary flow is heated by the electric heater. This is accomplished by diverting some of the flow downstream of the secondary venturi through a chocked orifice plate. The heated air is then remixed with the unheated air prior to entering the secondary air muffler and on through the coaxial piping entering the acoustic wind tunnel. The electric heater is capable of heating 1.25 lb/sec of air to 1100 deg. F.

3.3 MODEL NOZZLES TEST SETUP

Figures 5 and 6 show the front and side view of the 1/15 scale UHBR model nozzles installed in the open jet tunnel. Also shown in the Figures is the 36–inch diameter nozzle which provides the airflow for simulating the forward flight effects on the UHBR nozzles. The coaxial pipings that carry the primary and secondary air to nozzles are supported by a truss anchored to the concrete floor. This truss is approximately 156 inches upstream of the secondary nozzle exit plane. Upstream of the anchored/tiedown point is a stainless steel bellow which allow the coaxial pipings to grow and contract freely. Downstream of the anchored point, the coaxial pipings and the installed nozzles are canterlevered. In the course of the tests, the axial thermal expansion is calculated to be as much as 1.3 inches for the higher temperature primary core piping and 0.3 inches for the secondary. In the initial model nozzle design, two different length spacers were provided, one for cold flow operation and the other for hot flow operation. The secondary model nozzle also has three centering studs for controlling the coaxial nozzle concentricity. One of the studs was to be backed off before the start of the test to allow for the primary nozzle axial thermal growth. However, during the test rig shakedown both remaining centering studs were bent and the studs created a high frequency tone which was significantly higher than the tunnel background noise. For the actual noise test, the studs were eliminated and the holes in the secondary nozzle were filled. Without the centering studs, the coaxial nozzle has a 3.5% eccentricity (tilted toward 8'o clock).

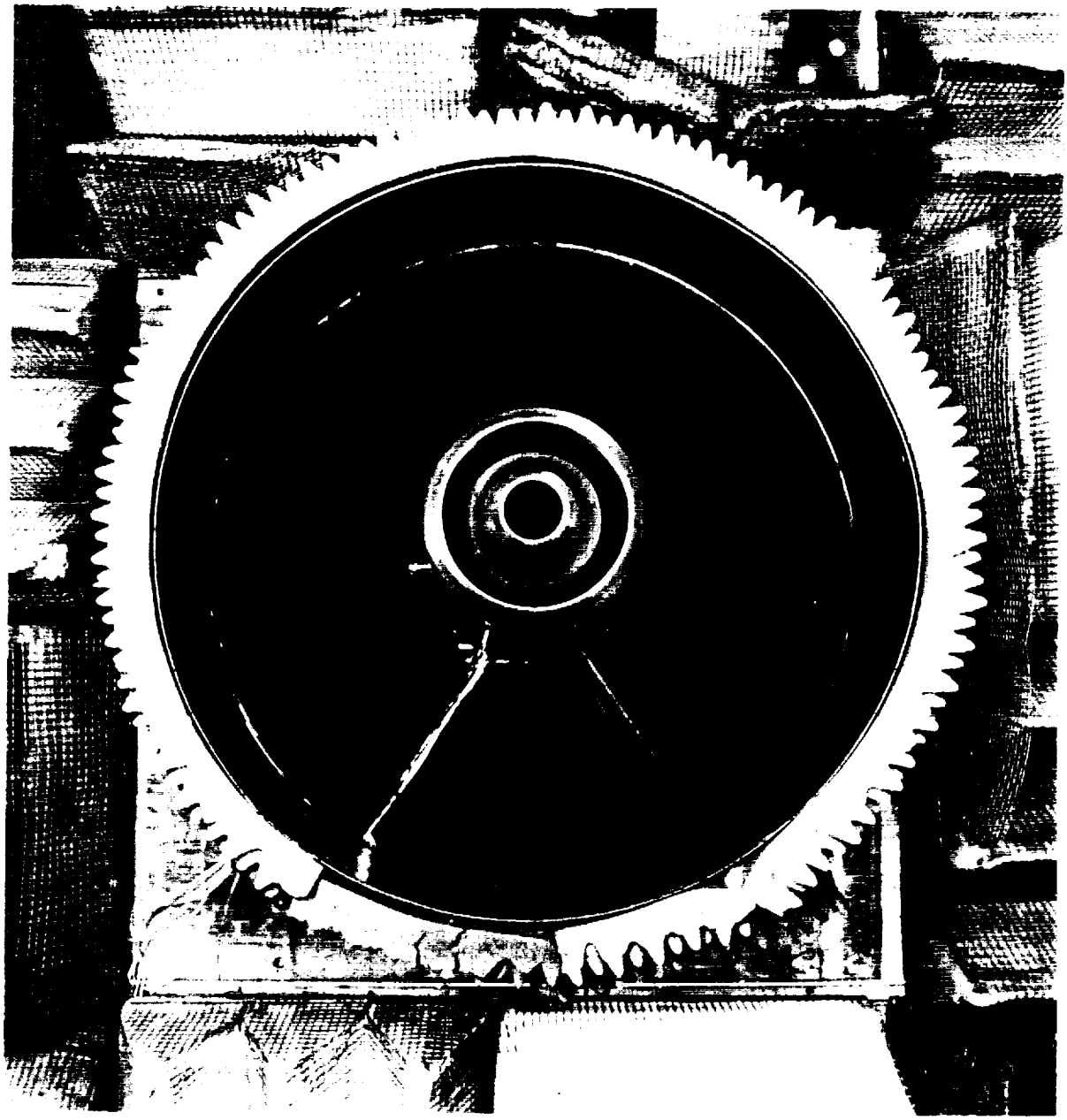

Figure 5. Front View of the 1/15–Scale UHBR Model Nozzles Installed in the FreeJet Tunnel.

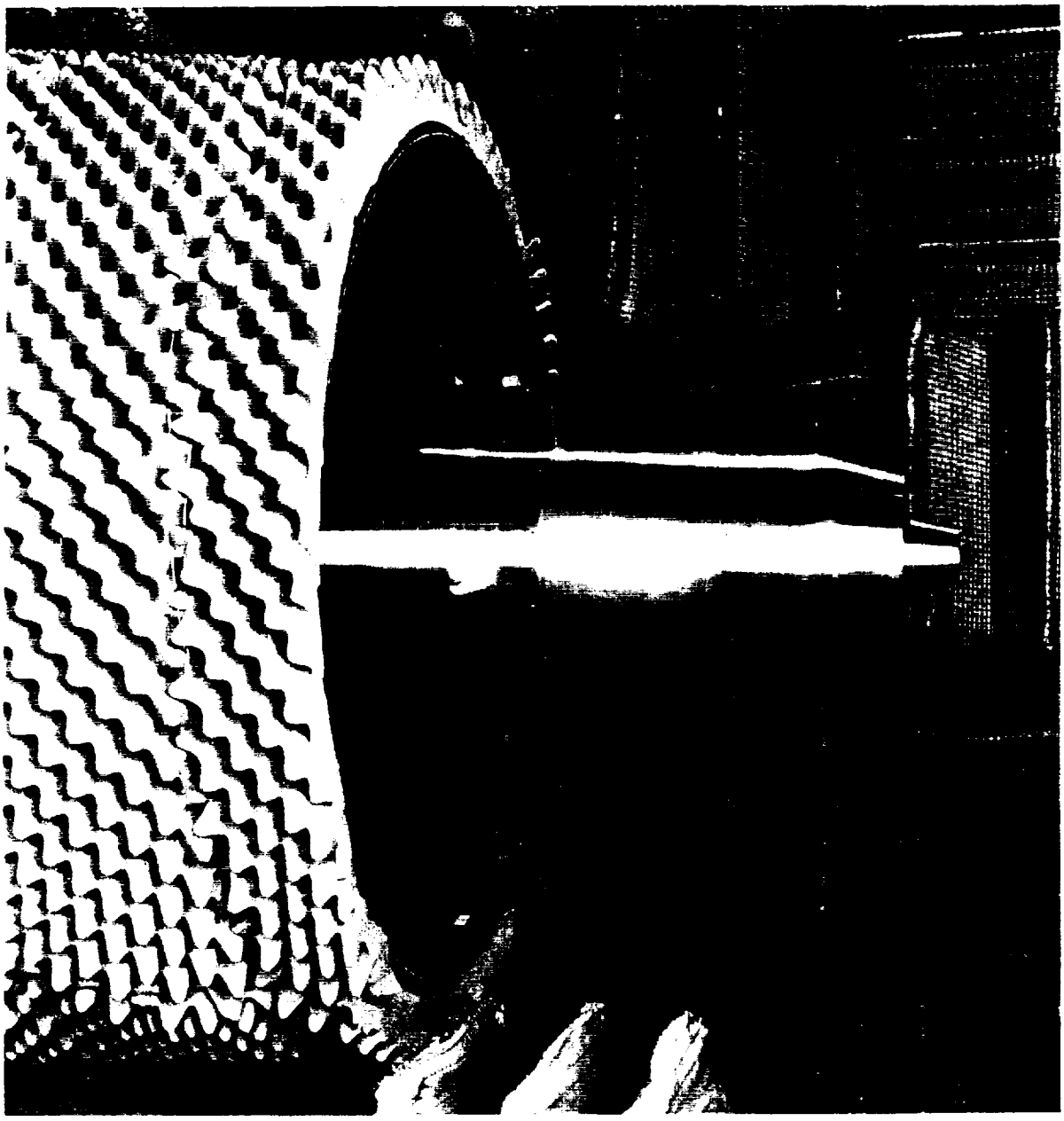

Figure 6. Side View of the 1/15–Scale UHBR Model Nozzles Installed in the Freejet Tunnel.

3.4 ACOUSTIC MEASUREMENTS SETUP

A schematic of the microphone locations for the noise test is shown in Figure 7. A total of 10 microphones were used for the test. These were placed at 80, 90, 100, 110, 120, 130, 135, 140, 145 and 150 degrees measured from the tunnel inlet axis. Microphones 80 through 135 degrees were placed on a sideline boom, 108 inches parallel to the centerline of the tunnel and 84 inches above the ground. The centerline of the UHBR model coaxial nozzle was 60 inches above the floor, thus the boom microphones were 24 inches higher than the nozzle centerline. The microphones were then tilted towards the nozzle centerline axis to provide a grazing orientation to the noise coming from the nozzle. This grazing angle orientation correction effectively lowered the microphone height from 84 to 81 inches. The slant distances for the microphones (80 through 135 degrees) were 113, 110, 113, 119, 128, 144 and 155 inches. The last three microphones (140, 145 and 150 degrees) were installed on a separate stand. These microphones were also orientated at grazing angle to the nozzle centerline axis. The effective heights and slant distances for these last three microphones are 81, 78, and 75 inches and 132, 123 and 117 inches, respectively.

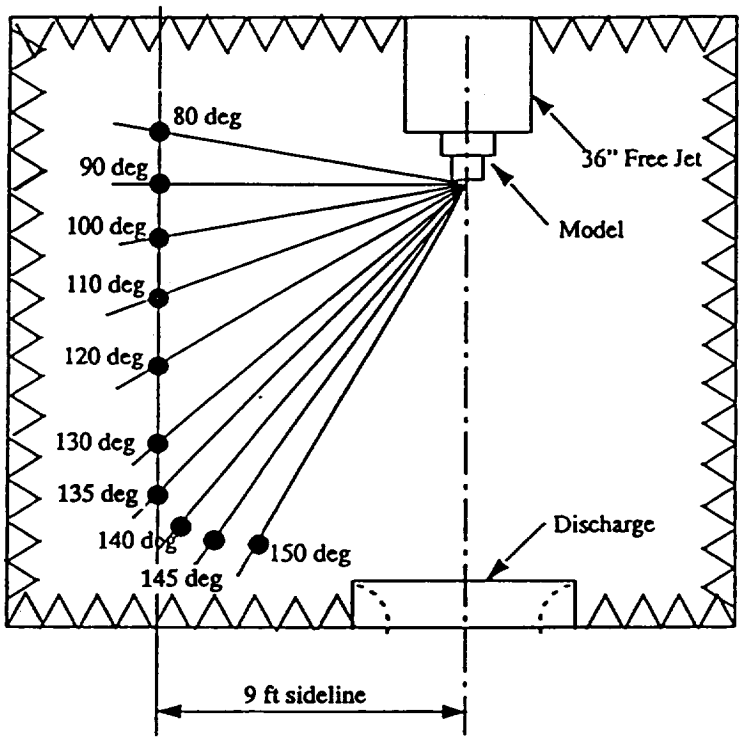

Figure 7. Schematic Showing Microphone Locations for the UHBR Jet Noise Test.

A picture of the microphone setup, the UHBR model nozzle, the 36–inch diameter nozzle for simulating forward flight effects and the anechoic chamber is shown in Figure 8.

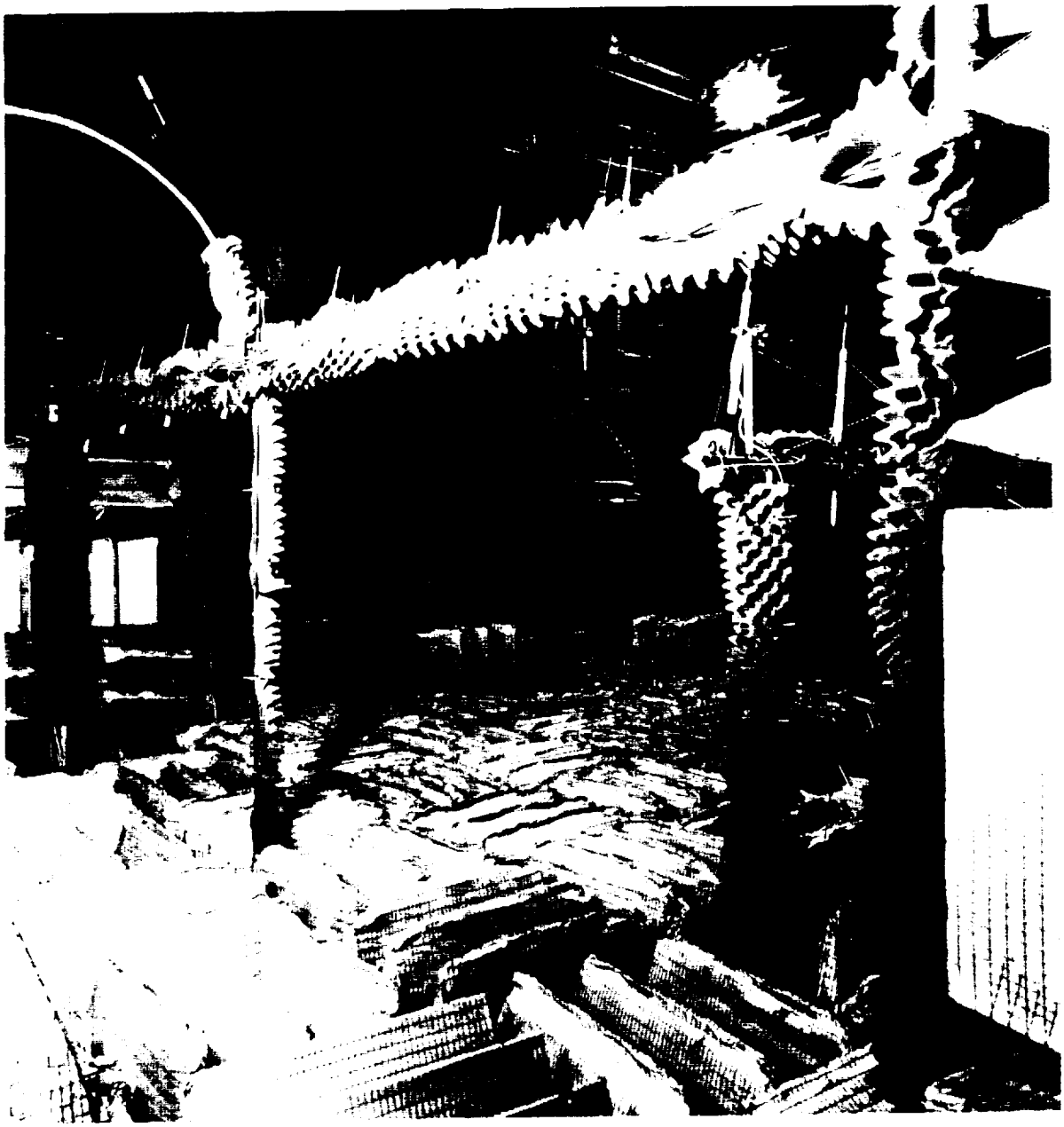

Figure 8. Microphones and Nozzles Test Setup in the UTRC Acoustic Research Tunnel.

3.5 INSTRUMENTATION

Instrumentations for acquiring performance data used in setting primary and secondary flow conditions for the UHBR model nozzle test matrix and for acquiring acoustics data are described below.

3.5.1 PERFORMANCE DATA

The performance data recorded for this UHBR model jet noise test are as follows:
(i) Atmospheric pressure and temperature,
(2) Primary (core) total temperature and total pressure approximately one (1) foot upstream of the nozzle exit,
(3) Secondary (fan) total temperature and total pressure approximately one (1) foot upstream of the nozzle exit,
(4) Chamber temperature, static pressure and relative humidity,
(5) Primary (core) flow venturi upstream temperature and pressure,
(6) Secondary (fan) flow venturi upstream temperature and pressure,
(7) Primary (core) flow venturi pressure drop,
(8) Secondary (fan) venturi pressure drop,
(9) Electric heater orifice plate upstream pressure and pressure drop across the plate,
(10) Wind tunnel screen pressure drop, and
(11) Open jet pressure drop.

Additional parameters that are important for the safe operation of the rig were monitored but not recorded. Thermocouples and pressure transducers used for the temperature and pressure measurements were directly interfaced to the data system via a Hewlett Packard (HP) 3497 Data Acquisition Control Unit. The data software system calculates and displays a set of preselected performance data on a On–line monitor. The test operator uses the On–line performance information to accurately set the test condition as specified in the test matrix. The calculated performance data is then printed out on hard copy. The calculated performance parameters that are considered important for this UHBR jet noise test are:
(a) Primary Jet Nozzle Pressure Ratio (NPR_{pri}),
(b) Primary Jet Total Temperature (T_{pri}) in deg. R
(c) Primary Jet Velocity (Vp or V_{pri}) in ft/sec,
(d) Primary Nozzle Area (A_{pri}) in sq.in,
(e) Primary Jet Mass Flow (M_{pri}) in lb/sec,
(f) Idealized Primary Mass Flow based on Primary Nozzle Area ($M_{pri\ ideal}$) in lb/sec,
(g) Primary Nozzle Discharge Coefficient (Cd_{pri}),
(h) Secondary Jet Nozzle Pressure Ratio (NPR_{sec}),
(i) Secondary Jet Total Temperature (T_{sec}) in deg. R,

(j) Secondary Jet Velocity (V_{sec}) in ft/sec,
(k) Secondary Jet Nozzle Area (A_{sec}) in sq.in.,
(l) Secondary Jet Mass Flow (M_{sec}) in lb/sec,
(m) Idealized Secondary Mass Flow based on Secondary Nozzle Area ($M_{sec\ ideal}$) in lb/sec,
(n) Secondary Nozzle Discharge Coefficient (Cd_{sec}),
(o) Idealized Fully Mixed Jet Velocity ($V_{m\ ideal}$) in ft/sec,
(p) Idealized Fully Mixed Jet Temperature ($T_{mix\ ideal}$) in deg.R,
(q) Idealized Fully Mixed Total Nozzle Area ($A_{mix\ ideal}$) in sq.in, and
(r) Wind Tunnel Mach Number (M_0) and/or Velocity (V_t) in ft/sec.

Figure 9 shows a picture of the Control Room of the UTRC Acoustic Research Tunnel where the test operator sets up the performance test conditions.

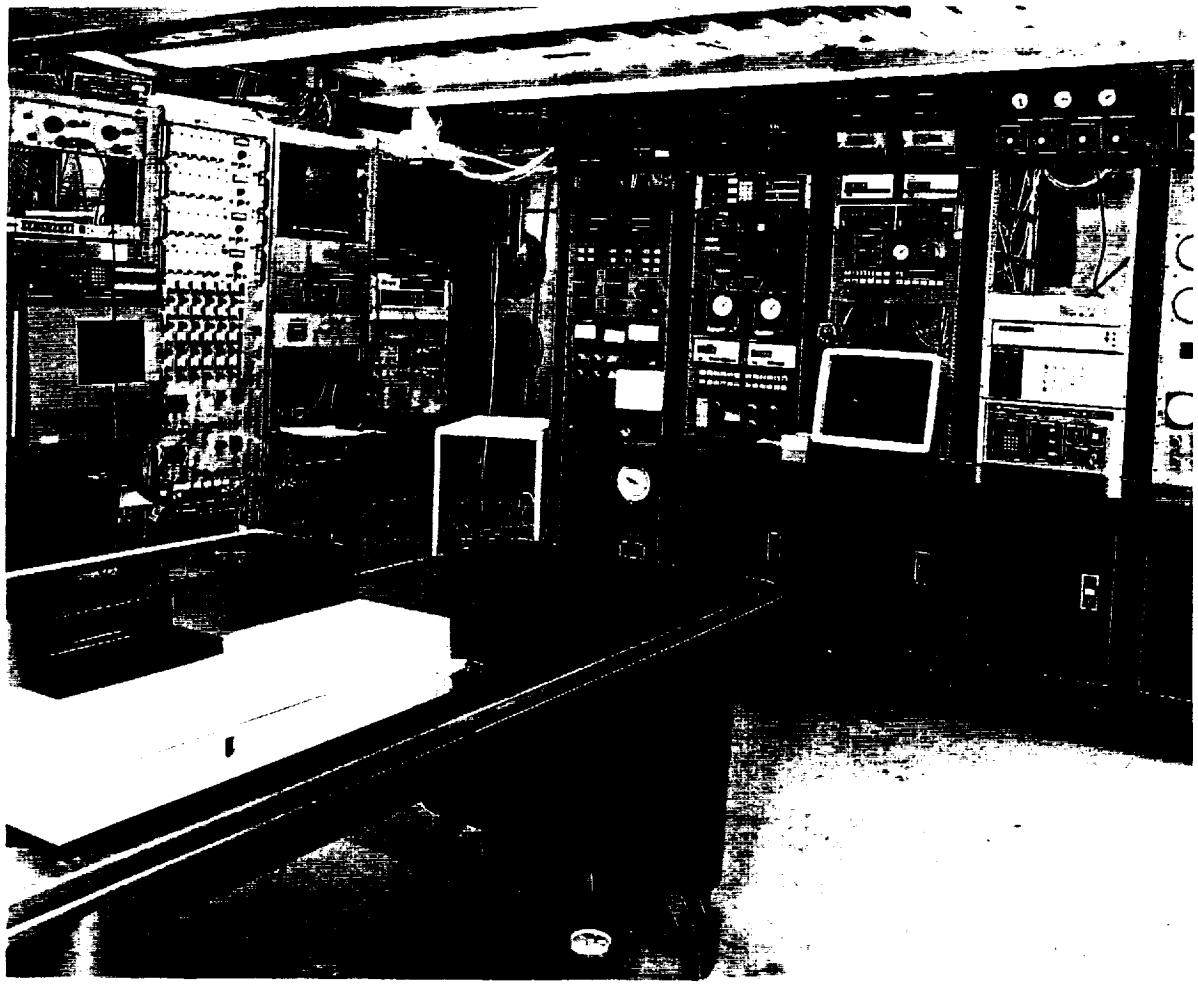

Figure 9. Control Room of the UTRC Acoustic Research Tunnel.

3.5.2 ACOUSTIC DATA

The microphones used in the UHBR jet noise test are 0.25–inch diameter B&K 4135 type grazing incident microphones with frequency responses that are essentially flat up to 80,000 hertz. The microphone grids (protecting the diagraphm) were removed prior to pistonphone calibration and remained off through the following noise test. The noise data were recorded and processed on–line using the Pratt and Whitney Multiple Analyzers Portable System (MAPS) shown in Figure 10. A further description of the MAPS is given in the DATA AQUISITION section.

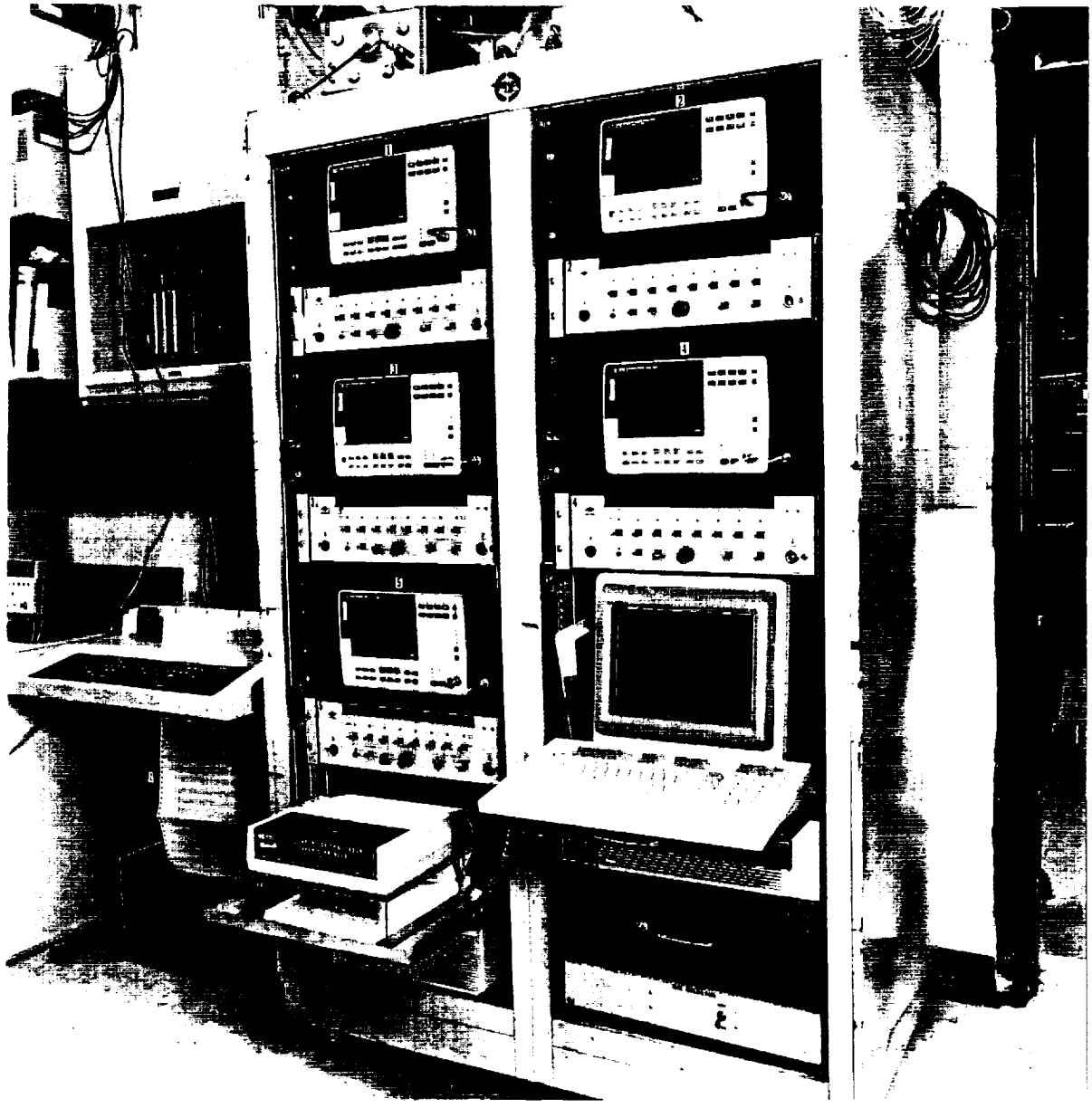

Figure 10. Pratt and Whitney's Multiple Analyzers Portable System (MAPS)..

3.6 NOZZLES AXIAL THERMAL GROWTH MEASUREMENTS

As described in Section 3.3, the coaxial pipings carrying the primary and secondary nozzles were anchored approximately 156 inches upstream of the nozzles exit planes. In an actual test condition, the primary (hot) piping, adaptor and nozzle could grow as much as 1.3 inch axially. The secondary (warm) piping, adaptor and nozzle grow at a lower rate. The relative axial positions of the primary and secondary nozzle exit planes are used in the calculation of the secondary nozzle area. A video camera was set up in the Anechoic test chamber to record the nozzle axial thermal growths under different primary–to–secondary temperature differences. A photo record of the nozzles thermal growths showing the relative axial spacings between the primary and secondary nozzle exit planes is shown in Figure 11 for four (4) temperature differences.

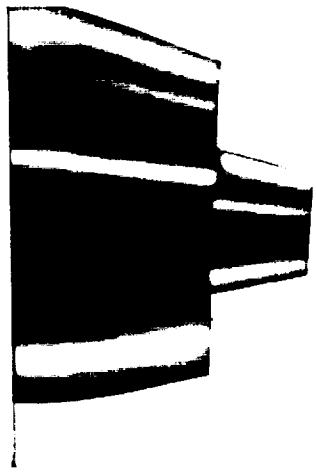

(a) Ambient (delta T = 0 deg. F)

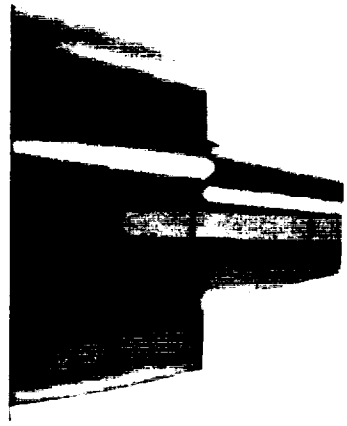

(b) delta T = 682 deg. F

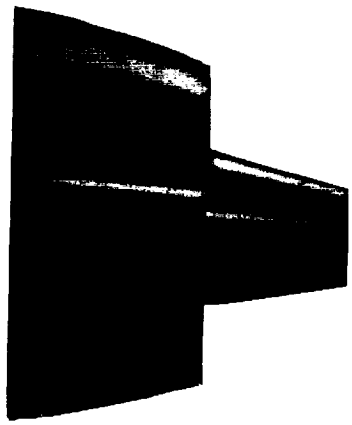

(c) delta T = 835 deg. F

(d) delta T = 880 deg. F

Figure 11. Axial Thermal Growth of Primary Nozzle Relative to Secondary Nozzle at Four (4) Temperature Differences.

The video camera's magnification and focus were adjusted so that the scale of the nozzle images displayed on the television monitor corresponded to the actual scale. A paper tape was pasted on the monitor and the relative positions of the nozzles exit planes at ambient temperature were marked. The axial spacing differences between the heated primary and the secondary nozzle exit planes were measured on the monitor as the primary core flow temperature was slowly increased along with the secondary flow temperature. The axial spacing data were then used to calculate the secondary nozzle areas. Figure 12 shows the correlation of the nozzle exits axial spacings and Figure 13 the correlation of the secondary nozzle areas as function of the temperature differences between the primary and secondary flows. The secondary nozzle area decreased from 29.6 sq.in at ambient condition to 26.8 sq.in at the highest UHBR jet temperature condition tested. Figure 13 is used for estimating the secondary nozzle area for each of the test point in the test matrix.

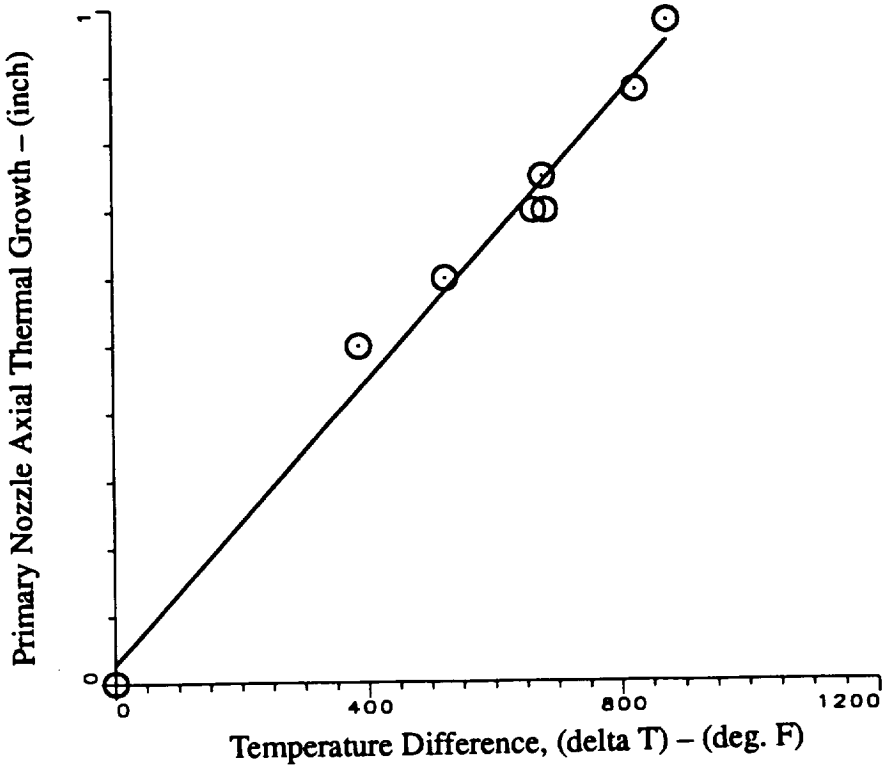

Figure 12. Correlation of the UHBR Primary–to–Secondary Nozzle Axial Growths with Temperature Differences Between Primary and Secondary Flow.

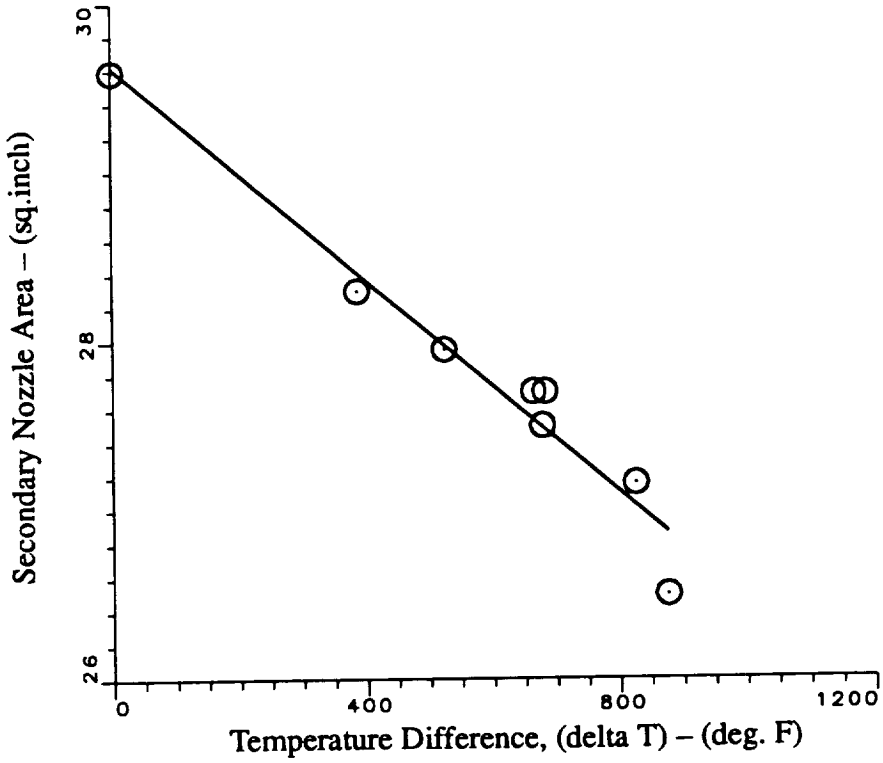

Figure 13. Correlation of the UHBR Secondary Nozzle Areas with Temperature Differences Between Primary and Secondary Flows.

4.0 DATA ACQUISITION AND REDUCTION

4.1 ACOUSTIC TEST MATRIX

The test matrix for the UHBR jet noise tests were selected to match exactly the flow conditions of the ADP demonstrator engine exhaust nozzle at seven power settings; 30%, 40%, 45%, 79%, 89%, 92% and 100% thrust. The test matrix is shown in Table 1.

Table1. Test Matrix for UHBR Jet Noise Tests at the UTRC ART.

Percent Thrust (%)	Primary NPR	Primary Temp. (deg. R)	Primary Velocity (ft/sec)	Primary Wt.Flow (lb/sec)	Secondary NPR	Secondary Temp. (deg. R)	Secondary Velocity (ft/sec)	Secondary Wt. Flow (lb/sec)
30	1.086	1237	589	0.416	1.089	555	400	4.92
40	1.117	1296	697	0.476	1.116	558	455	5.58
45	1.131	1315	740	0.500	1.130	563	481	5.89
79	1.260	1414	1044	0.705	1.232	579	634	7.66
89	1.307	1438	1130	0.767	1.259	581	667	8.11
92	1.321	1462	1161	0.780	1.266	582	675	8.25
100	1.361	1504	1237	0.820	1.286	588	700	8.36

where NPR is the nominal Nozzle Pressure Ratio, and
Temp is the Total Jet Temperature.

The secondary nozzle areas were calculated from Figure 13 and are presented in Table 2.

Table 2. Calculated Values of Secondary Nozzle Areas, Bypass and Nozzle Area Ratios.

Percent Thrust (%)	Primary Nozzle (sq.in)	Secondary Nozzle (sq.in)	Pri. Noz Discharge Coefficient	Sec. Noz. Discharge Coefficient	Bypass Ratio	Nozzle Area Ratio
30	3.75	27.7	0.83	0.87	11.83	7.39
40	3.75	27.6	0.83	0.87	11.72	7.36
45	3.75	27.5	0.83	0.88	11.79	7.33
79	3.75	27.2	0.87	0.88	10.86	7.25
89	3.75	27.0	0.88	0.88	10.56	7.20
92	3.75	26.9	0.88	0.88	10.32	7.17
100	3.75	26.7	0.89	0.89	10.22	7.12

The nozzle pressure ratios and jet total temperatures listed on Table 1 were nominal values. Actual values were recorded at each test condition and were generally within a few percent of the nominal target values. The nozzle discharge coefficients (Cd) for the primary and secondary nozzles were calculated from the actual measured mass flow rates and the idealized mass flow rates for the measured physical nozzle areas. These discharge coefficient values were of the order of .83 to .89 for the primary nozzle and from .87 to .89 for the secondary nozzle, indicating that the secondary jet had significant influence on the discharge rate of the primary jet and vice versa. Noise data were recorded for the above test matrix at four wind tunnel Mach numbers; 0.0, 0.2, 0.27 and 0.35. Each test point were repeated at least once. Background wind tunnel noise data at each Mach number were recorded.

4.2 ACOUSTIC SIGNAL PROCESSING AND RECORDING

At the start of the test day, the microphones were calibrated with a B&K Type 4220 pistonphone which generated a 124 dB tone at 250 Hertz. After pistonphone calibration, the acoustic signals from the microphones were then passed through 200–Hertz high–pass filters to eliminate the low frequency portion of the noise spectra associated with the wind tunnel fan drive system. (200 Hertz 1/15 model scale is equivalent to 13 Hertz for the full–scale UHBR Nozzle). The signals were then conditioned through preamplifiers and teed off into the Pratt and Whitney's Multiple Analyzers Portable System (MAPS) and into an analog recorder (RACAL) with the noise data stored on a magnetic tape. The sole purpose of the tape was provide to a backup system in the unlikely event that the MAPS signal processing failed during the noise test. MAPS was the primary acoustic data processing system for the noise test. The MAPS system was comprised of two 6–foot tall standard instrumentation bays which contain up to 40 microphone channels (power supplies, switching, gain normalization, etc) controlled by a small computer. Signals from the microphones were connected in sets of five (5) to five (5) B&K Type 2811 (8–Channel) Multiplexers, and then onto five (5) Hewlett Packard Type 3651A Single Channel Analyzer. Once the MAPS system was calibrated, the computer assumed the sequencing and real time processing of five (5) microphone data at a time until all microphone signals were completed. The noise spectral results from the analyzers (in the form of thirty three (33) 1/3–octave band sound pressure levels (SPLs) from 50 Hertz to 80,000 Hertz.) were stored on a computer disk. Additional heading informations (Run Number, relative humidity, temperature, tunnel Mach number, etc.) were added to the data record immediately after each test point. At the end of each test day, post calibrations of the microphones were conducted and any variation between the pre– and post–calibrations were recorded. The stored noise data were corrected for microphone responses, system gains/losses, system frequency responses, and atmospheric absorption for actual test day temperature and relative humidity, and transmitted to the Pratt and Whitney's Engineering Mainframe Computer, where further data corrections and reductions are processed.

4.3 ACOUSTIC DATA REDUCTION

Further adjustments were made to the acoustic data stored in the mainframe computer. These were (1) subtracting wind tunnel background noise from the data, (2) applying a shear–layer refraction correction to the data, (3) subtracting out the (incorrect) atmospheric absorption correction from MAPS which assumed a common radius for the microphones, and applying the correct atmospheric absorption corrections for each microphone based on the microphone's individual slant distance, and (4) scaling the model data results to fullscale and extrapolating the results to 150–foot radius distance for comparison with fullscale ADP demonstrator engine noise data.

4.3.1 ACOUSTIC WIND TUNNEL BACKGROUND NOISE

Figure 14 shows plots of the wind tunnel background noise levels measured at different microphone locations for three (3) tunnel Mach numbers; 0.2, 0.27 and 0.35. (The background noise levels for the no tunnel flow condition were significantly lower and off the scales of Figure 14.) The spectra shown in Figure 14 had been "shifted" by four (4) octaves to show how the tunnel data would impact the fullscale spectra of the UHBR jet noise data.

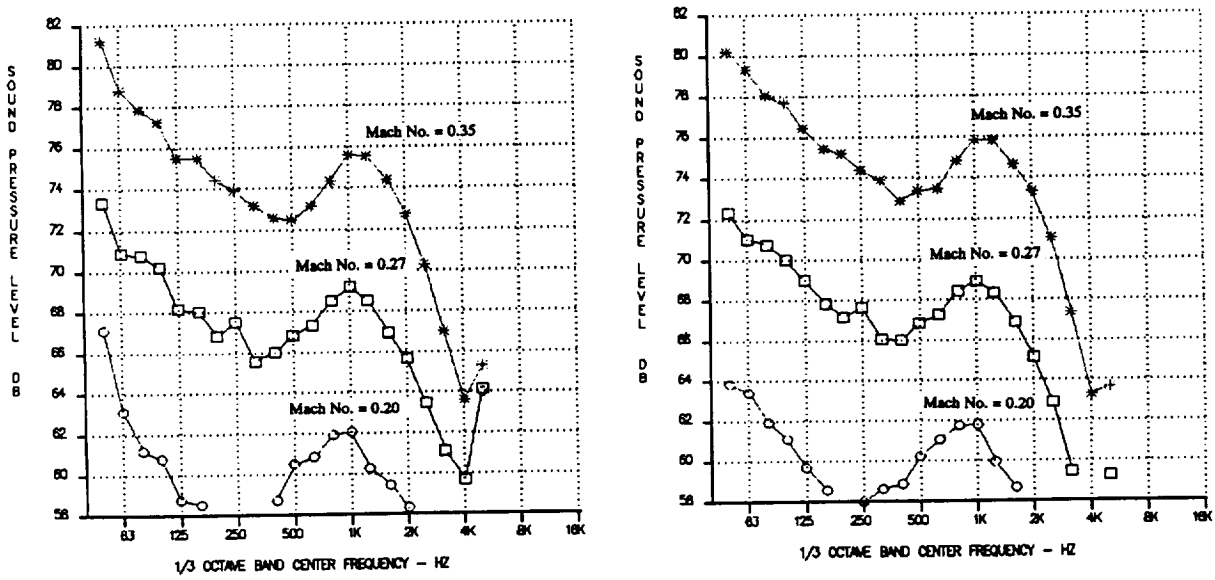

(a) Tunnel Noise at 80 degrees.

(b) Tunnel Noise at 90 degrees.

Figure 14. Wind Tunnel Background Noise Levels Measured at Different Microphone Locations for Tunnel Mach Numbers, 0.20, 0.27 and 0.35.

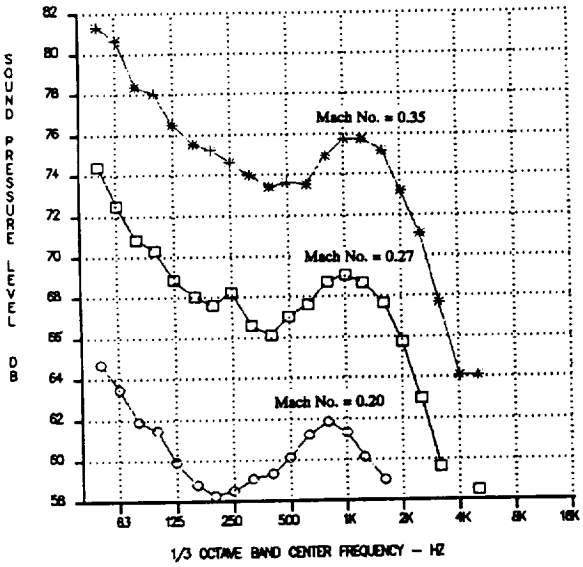

(c) Tunnel Noise at 100 degrees

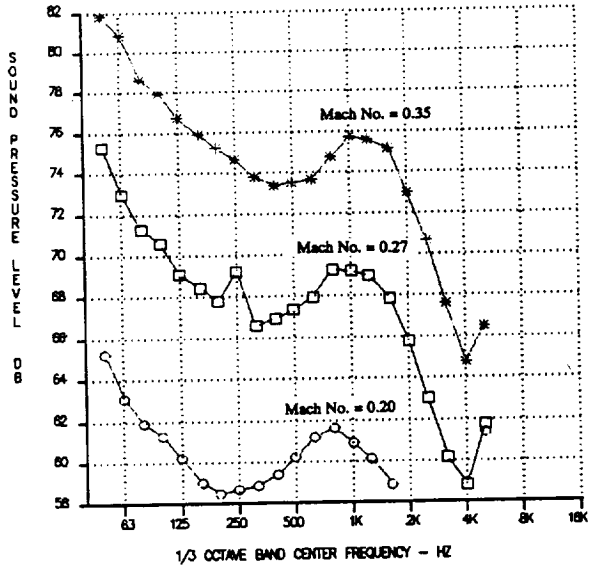

(d) Tunnel Noise at 110 degrees

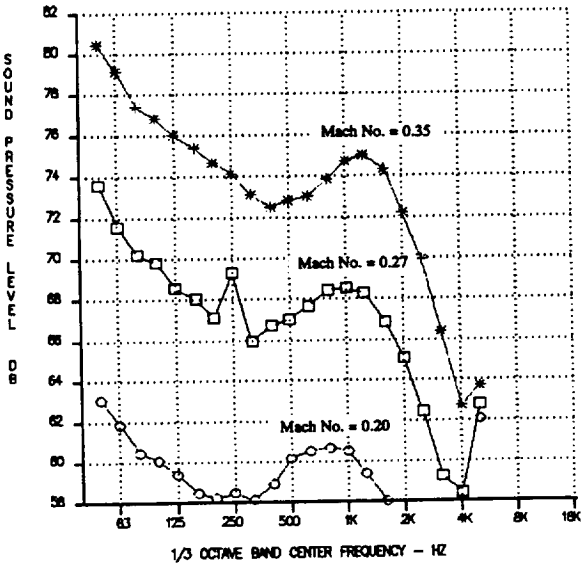

(e) Tunnel Noise at 120 degrees

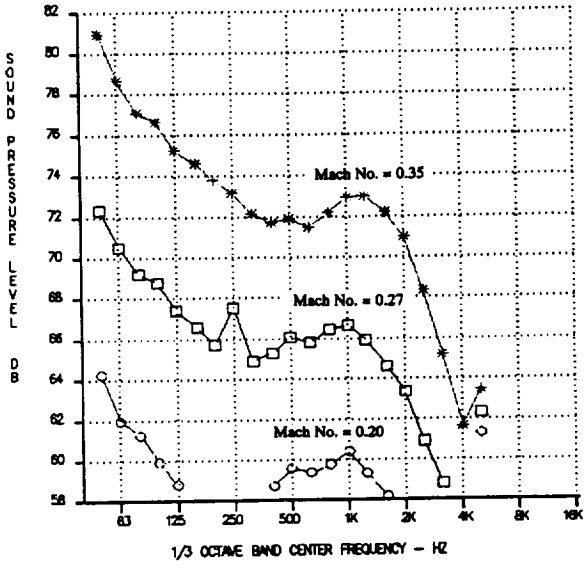

(f) Tunnel Noise at 130 degrees

Figure 14. (cont) Wind Tunnel Background Noise Levels Measured at Different Microphone Locations for Tunnel Mach Numbers, 0.20, 0.27 and 0.35.

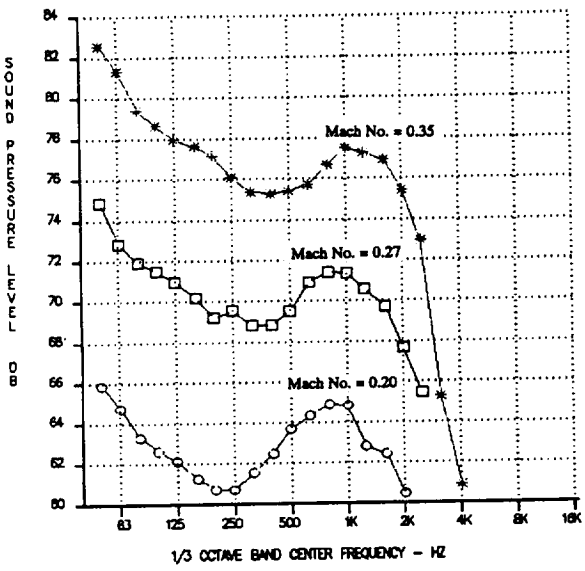

(g) Tunnel Noise at 140 degrees

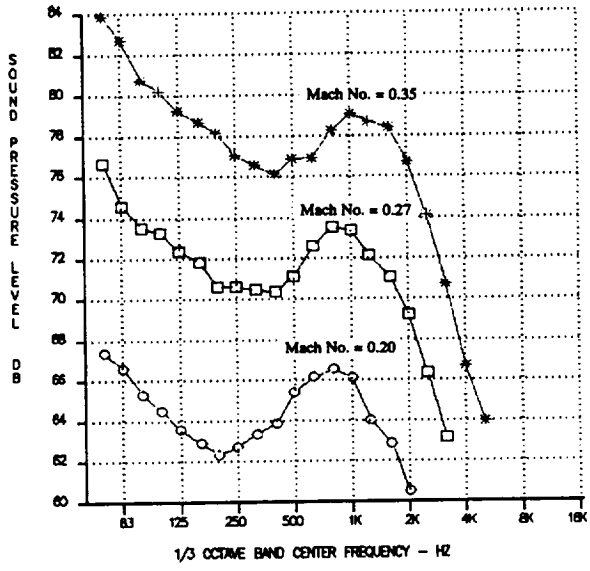

(h) Tunnel Noise at 150 degrees

Figure 14. (cont). Wind Tunnel Background Noise Levels Measured at Different Microphone Locations for Tunnel Mach Numbers, 0.20, 0.27 and 0.35.

The 0.35 Mach number background data was found to be significantly higher than the UHBR jet noise at six (6) of the seven (7) test conditions. The only useful data for the 0.35 Mach number point was the 100 % (ADP engine) thrust test point. The 0.27 Mach number tunnel background data was higher than the UHBR jet noise at three (3) of the seven (7) test conditions. The useful data for the 0.27 Mach number point were the 79%, 89%, 92% and 100% thrust test points. Similiarly, the useful data for the 0.20 Mach number point were 45%, 79%, 89%, 92% and 100% thrust test points. The criteria that was used to decide whether or not to process the data for a test point was that the "total" jet plus tunnel background noise must be at least 3 dB higher than the tunnel background noise. For those data points that met the criteria, background noise were subtracted (logarithmically) from the acoustic data.

4.3.2 FREE–JET SHEAR LAYER REFRACTION CORRECTION

The shear layer refraction correction accounts for the jet noise refraction by the free–jet shear layer. Sound propagating through the shear layer is refracted and changed in amplitude. A detail thereoretical discussion of the shear layer refraction correction is presented in Roy Amiet's AIAA Paper 75–532, 1975, (Ref. 1). The software program written specifically for the UTRC ART free–jet shear layer correction has been ultilized in every past jet noise experiments con-

ducted in the UTRC ART facility. Data corrected by this method is equivalent to measurements taken taken by a microphone moving with the jet as in forward flight. A second correction known as a "moving medium or tunnel flow" correction is then applied which will transform the measurements to a fixed frame microphone system with the jet moving at the tunnel Mach number. To do this, the shear layer corrected angle must be corrected back to the retarded angle of noise emission where the source was first emitted.

A detailed description of the procedure and sample calulations of the magnitudes of the angles and amplitude corrections for this UTRC ART facility can be found in (Section 4.2) of Reference 2.

4.3.3 ATMOSPHERIC ABSORPTION CORRECTIONS

The acoustic data transmitted from MAPS to the Pratt and Whitney Engineering Mainframe Computer contained incorrect values for atmospheric absorption corrections. MAPS assumed that the microphones distances were at constant radius and thus the corrections applied were incorrect for this UHBR jet noise test where the microphones were placed at different slant distances from the primary nozzle exit. These incorrect values were subtracted from the data and the correct atmospheric absorption values based on each individual microphone slant distance were applied. The equations for the abssorption coefficients (per 1000 foot distance) for frequencies 50 through 80,000 Hertz used for this test were adapted from the University of Mississippi, Reference 3. The acoustic data were then normalized to a one (1) foot radius by applying the spherical divergence correction for each individual microphone based on the microphone's slant distance. The model data can then be scaled to fullscale (for nozzle size) and extrapolated to any distance in the far–field. The atmospheric absorption corrections based on the fullscale jet frequencies and extraploated distances, and calculated for the standard "acoustical day", 77 deg.F and 70% relative humidity are then applied to the full–scaled UHBR jet noise data for direct comparison with data taken from the ADP demonstrator engine.

4.3.4 NOISE RESULTS SCALED TO FULLSCALE AND EXTRAPOLATED TO 150–FOOT RADIUS FOR COMPARISON WITH ADP DEMONSTRATOR ENGINE DATA

The scaling of the 1/15–scale model jet noise data to fullscale ADP engine was accomplished by shifting the model jet noise spectra down twelve (12) one–third octave freqency bands, and adding 10 log(scale factor) which is 11.76 dB to all the levels. The 80,000–Hertz 1/3 octave band of the model jet noise spectra became the 5,000–Hertz 1/3 octave band of the full–scaled jet noise spectra. The resulting full–scaled jet noise spectra, therefore, had missing values for the 6,300,

8,000 and 10,000 Hertz bands. The missing values were "filled" in using an assumed jet noise high frequency rolloff rate of 1 dB per 1/3 octave band. Some of the full–scaled data also had "rollups" where the levels for the 5,000 Hertz bands were higher than those for the 4,000 Hertz bands. These rollups were eliminated by assuming the same rolloff rate of 1 dB per 1/3–octave band for the 5,000 Hertz band. The resulting fullscale data were then extrapolated to 150–foot radius using the corrections for spherical divergence and for atmospheric absorptions for the additional extrapolated distance.

5.0 RESULTS AND DISCUSSIONS

5.1 UHBR JET NOISE DATA REPEATABILITY

Figure 15 shows a sample comparison plot of the data from three repeat runs. The data scatter from run to run is approximately 0.5 dB and in general the scatter is less at the most aft angles, 130 through 150 degrees.

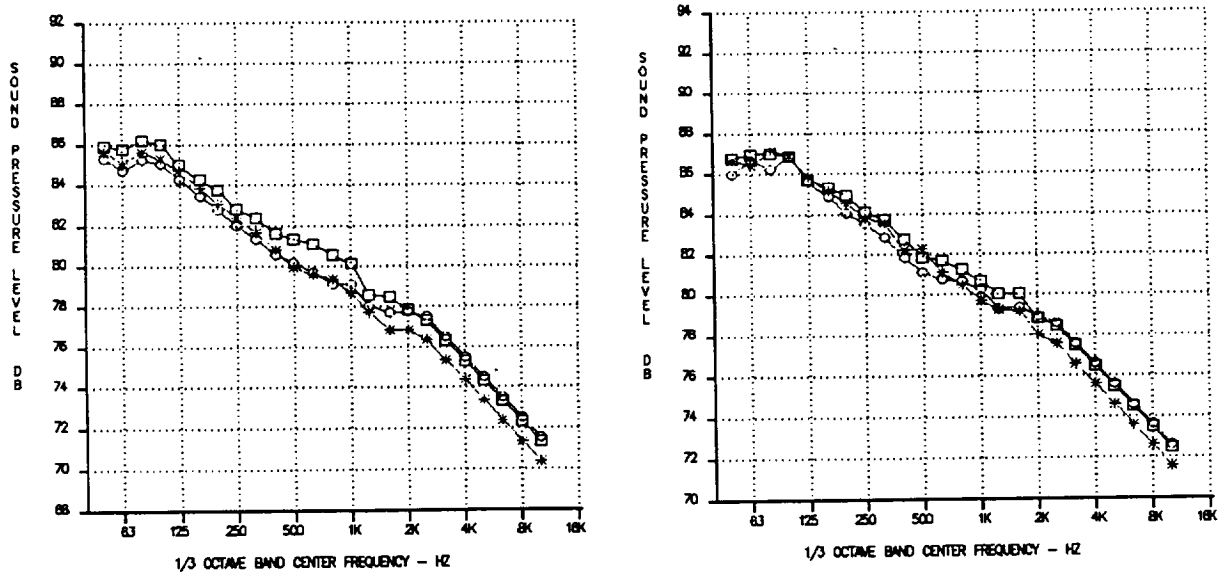

(a) 90 degrees

(b) 100 degrees

Figure 15. Spectral Comparisons Showing Jet Noise Data Repeatability from Three Runs.

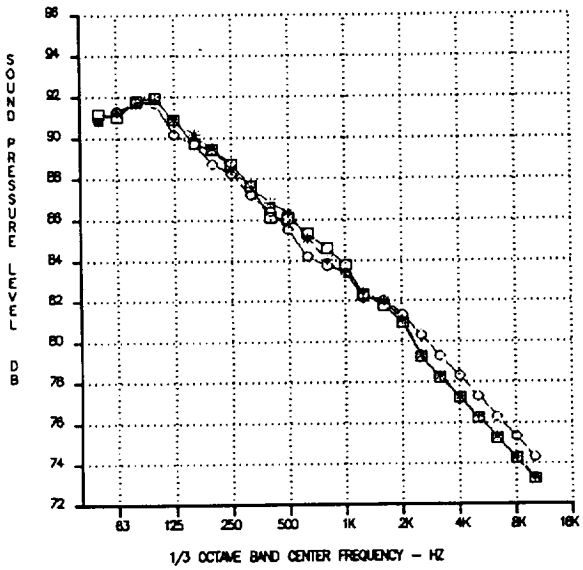

(c) 120 degrees

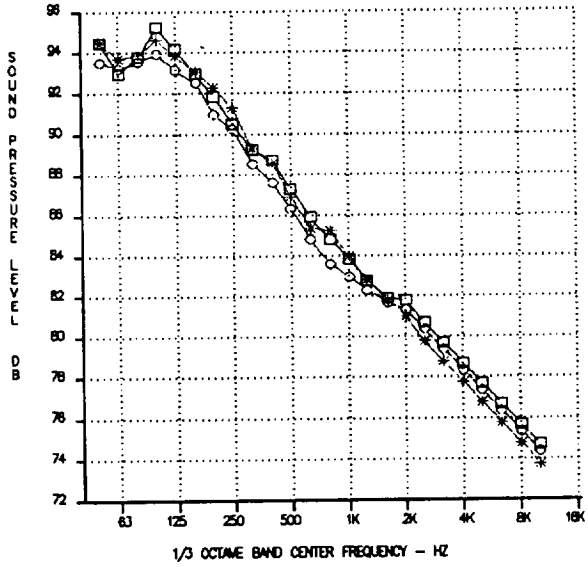

(d) 130 degrees

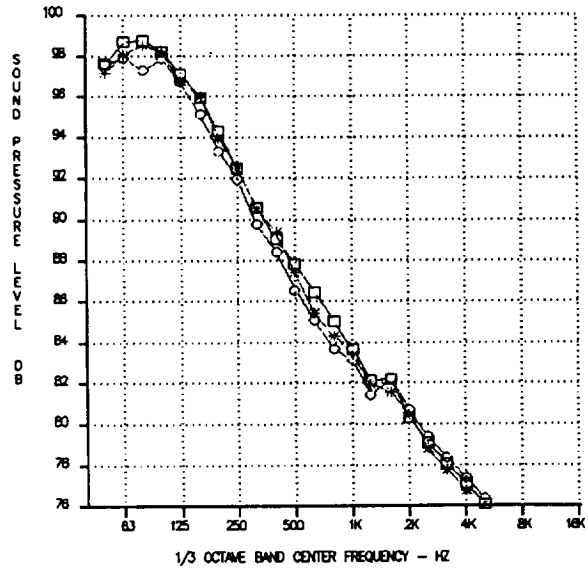

(e) 140 degrees

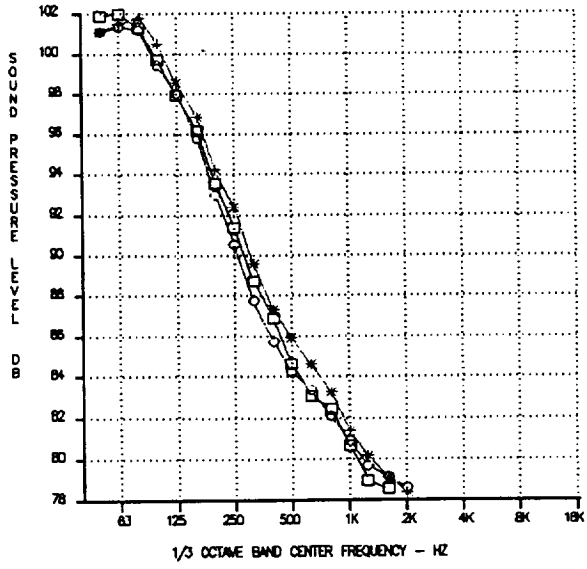

(f) 150 degrees

Figure 15. (cont). Spectral Comparisons Showing Jet Noise Data Repeatability from Three Runs.

5.2 COMPARISONS WITH ADP ENGINE DATA

Figures 16 through 22 show spectral comparisons of the averaged UHBR jet noise with ADP engine data for the seven (7) ADP power settings tested. Also shown in the Figures are the predicted levels of fan and core noise obtained by subtracting the jet from the total noise. The results show that the UHBR jet noise levels to be substantially lower than those of the fan and core noise for power setting up to 100 % thrust. Jet noise tends to dominate the very aft angle (150 degrees) while fan and core noise dominate the less aft angles and at most power settings. Tthese spectral comparisons indicate that the UHBR jet noise is not a major noise source for the ADP engine.

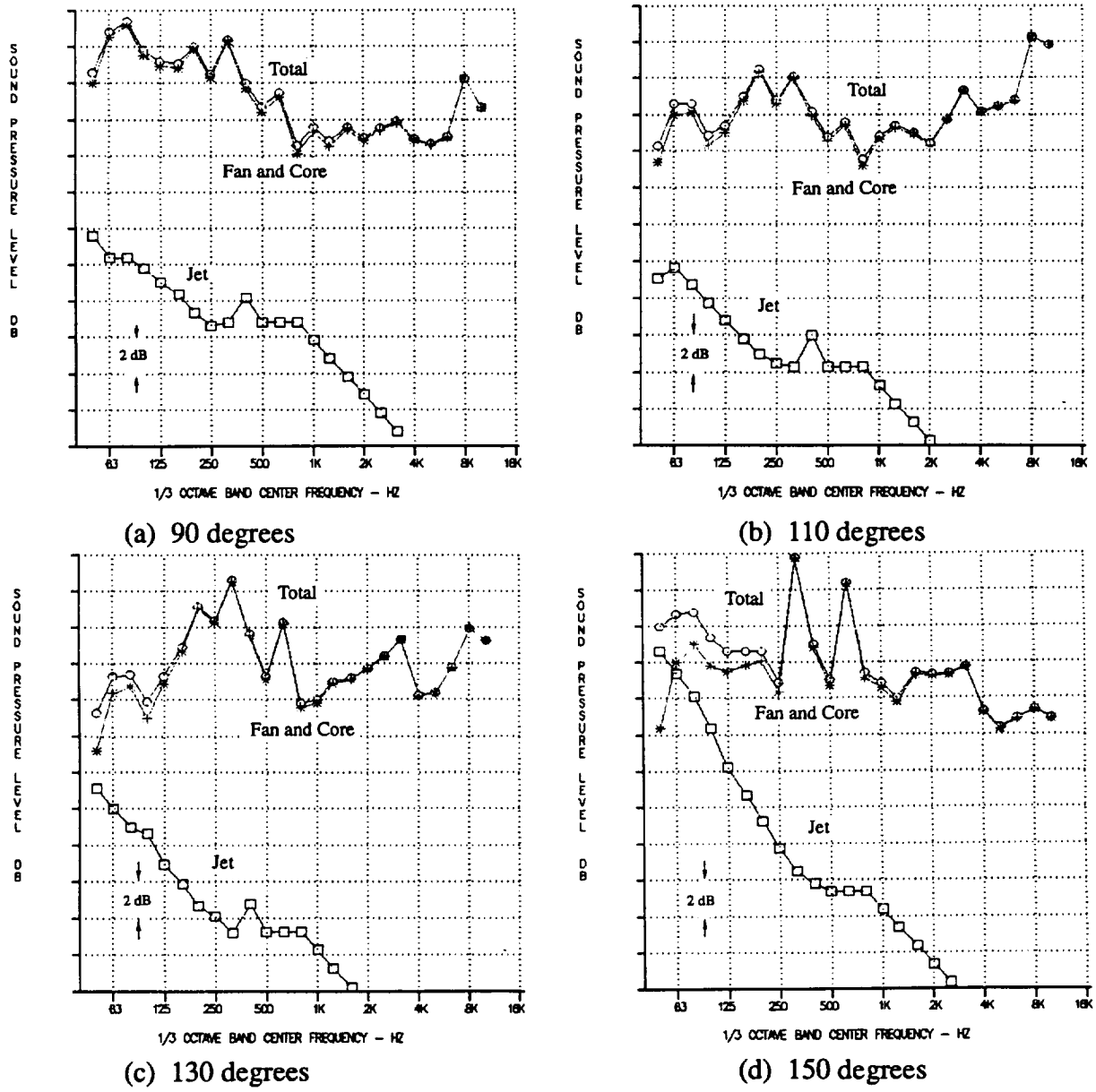

Figure 16. Spectral Comparisons of the UHBR Jet and the ADP Engine Noise at 30% Thrust.

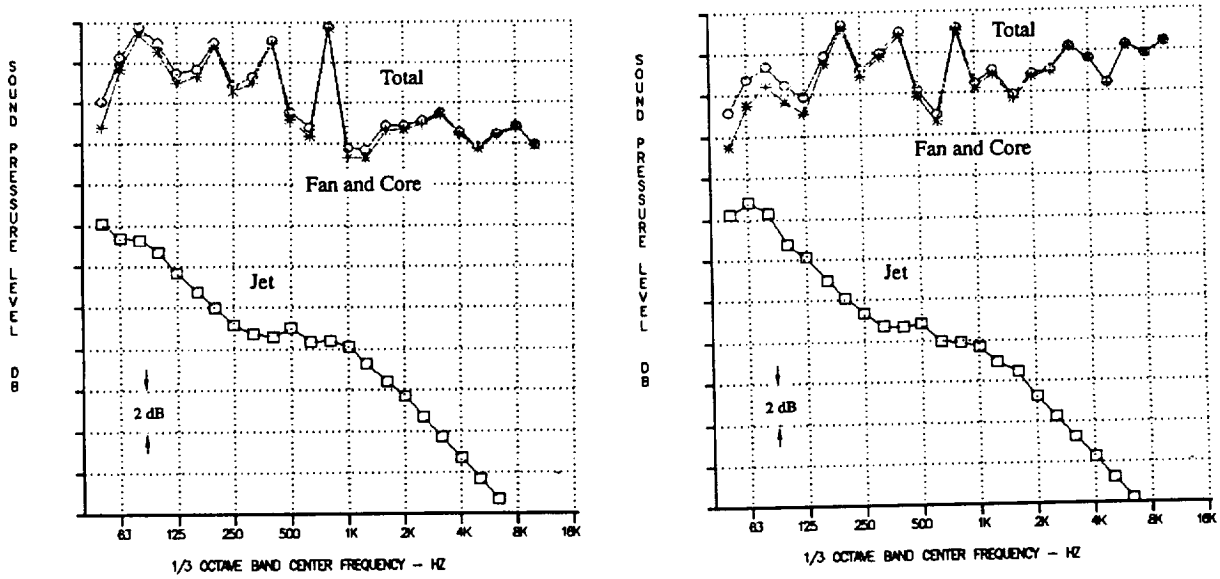

(a) 90 degrees

(b) 110 degrees

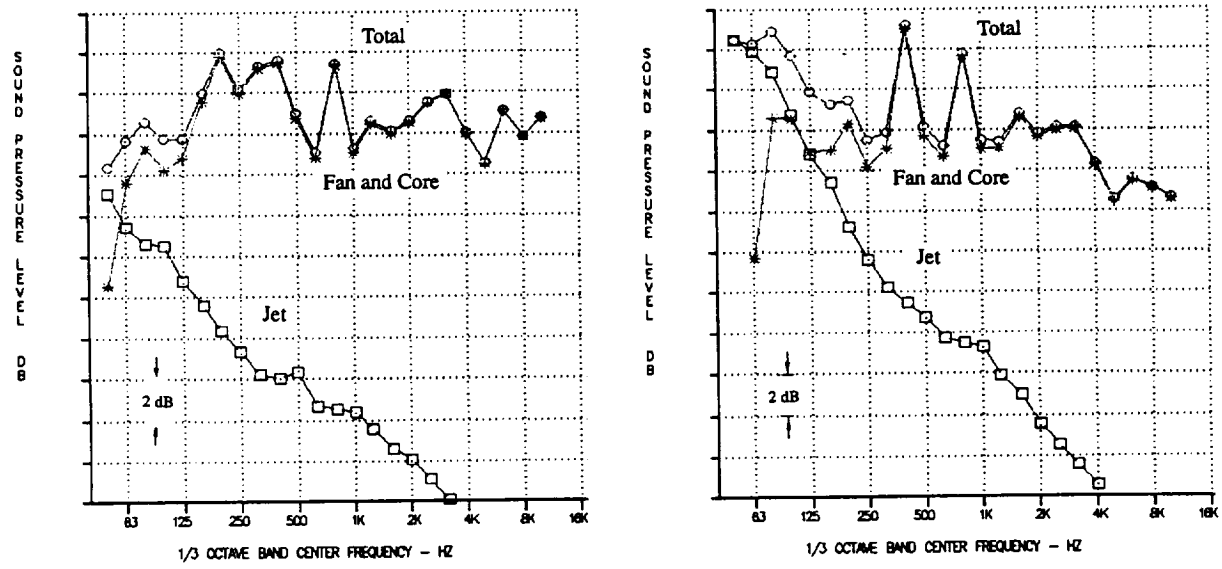

(c) 130 degrees

(d) 150 degrees

Figure 17. Spectral Comparisons of the UHBR Jet and the ADP Engine Noise at 40 % Thrust.

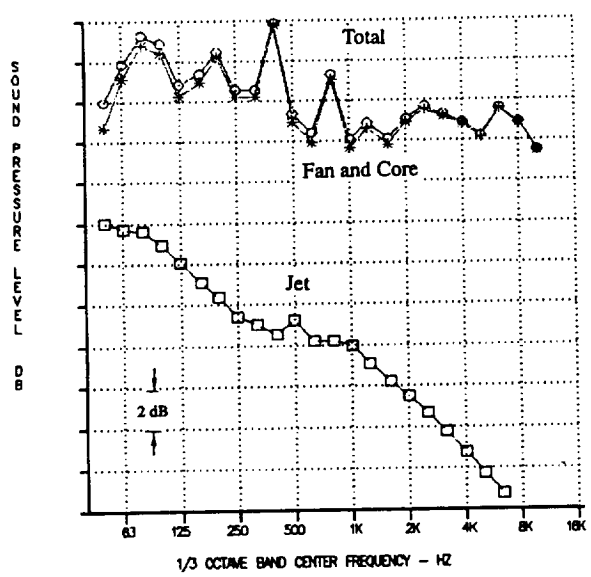

(a) 90 degrees

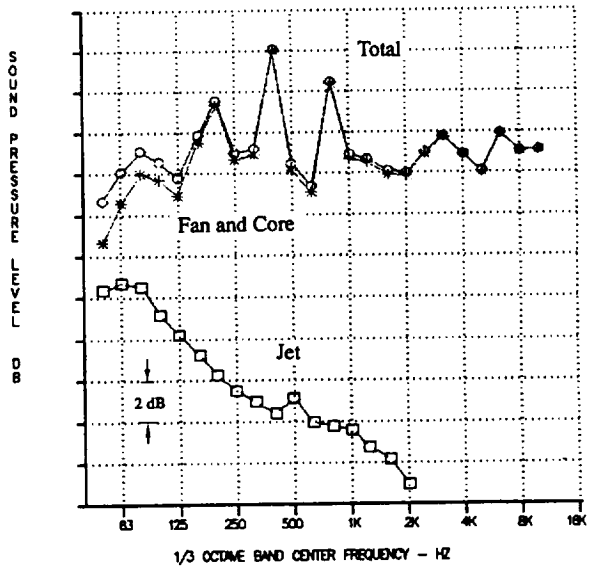

(b) 110 degrees

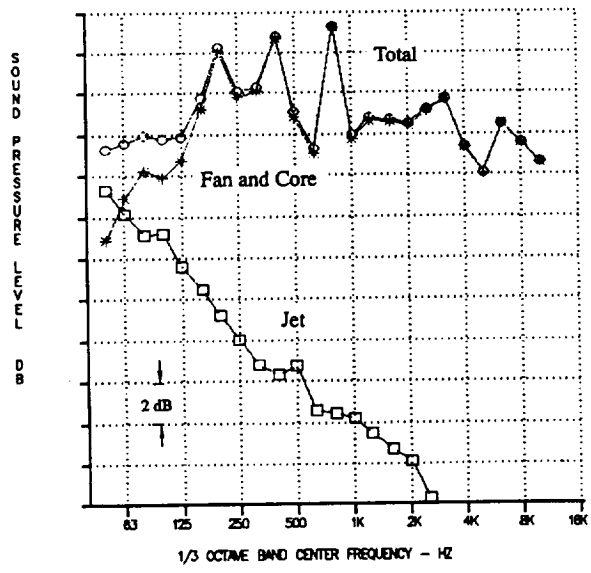

(c) 130 degrees

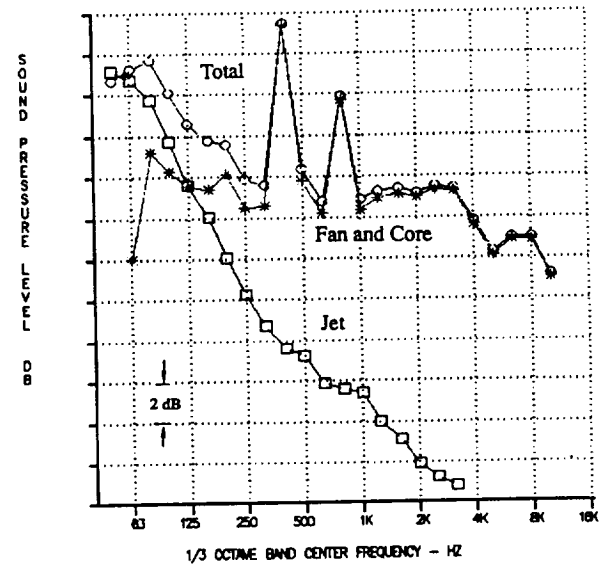

(d) 150 degrees

Figure 18. Spectral Comparisons of the UHBR Jet and the ADP Engine Noise at 45 % Thrust.

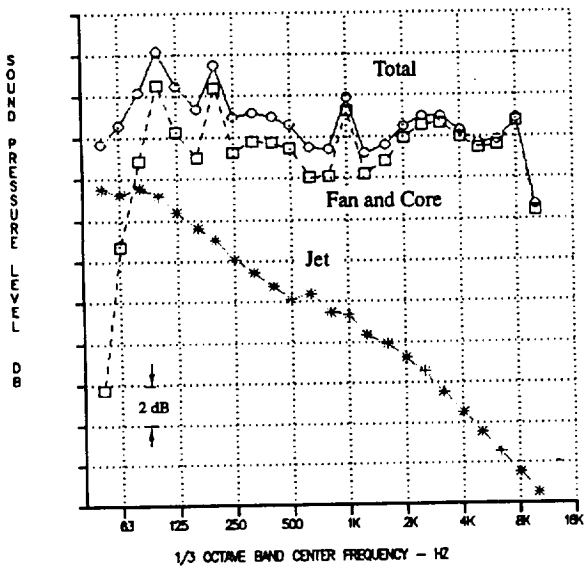

(a) 90 degrees

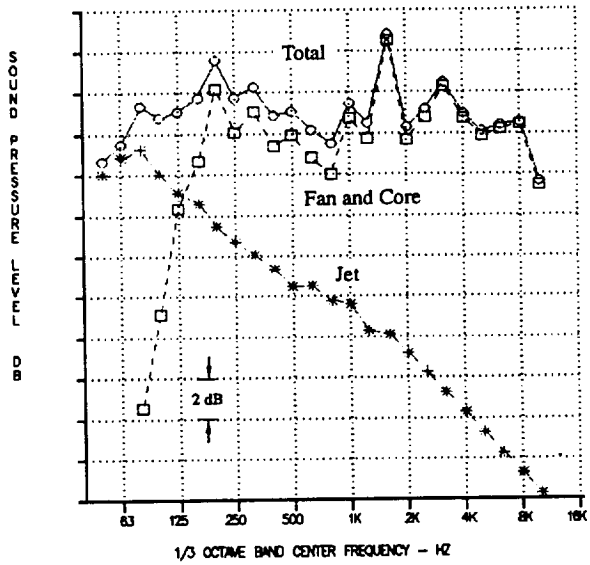

(b) 110 degrees

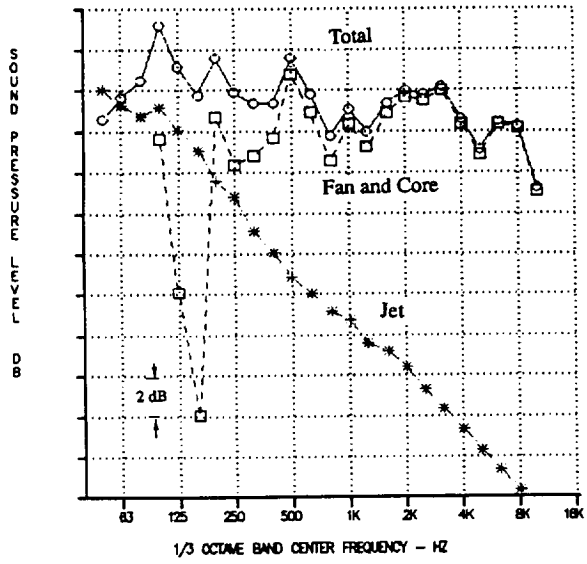

(c) 130 degrees

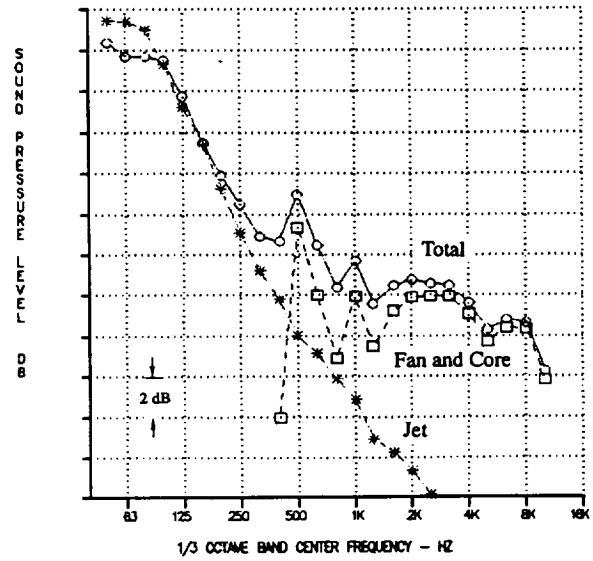

(d) 150 degrees

Figure 19. Spectral Comparisons of the UHBR Jet and the ADP Engine Noise at 79 % Thrust.

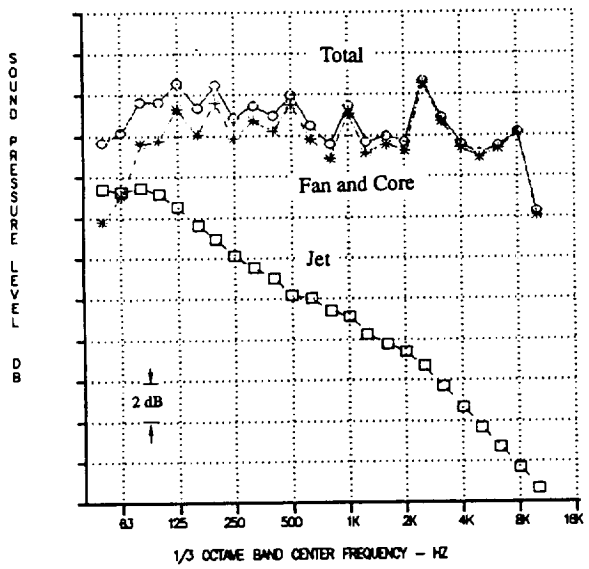

(a) 90 degrees

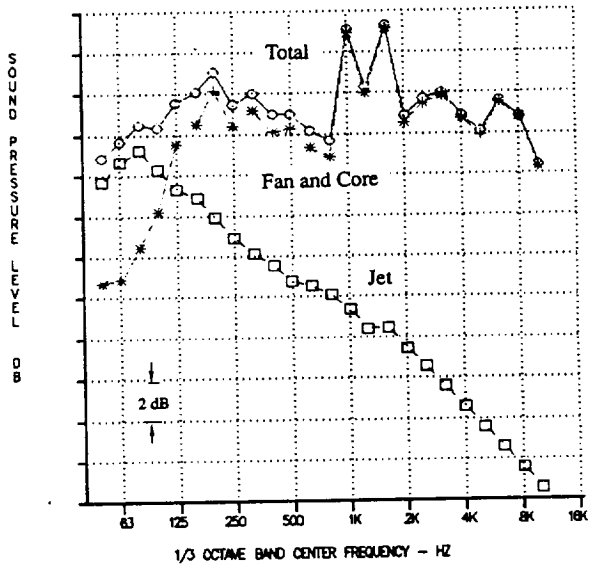

(b) 110 degrees

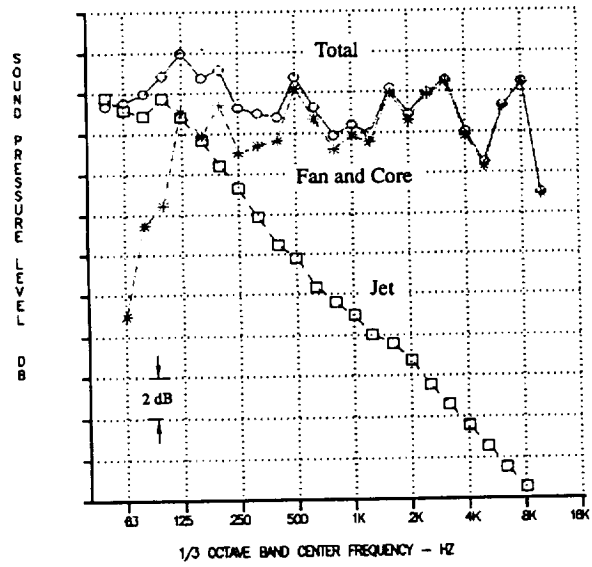

(c) 130 degrees

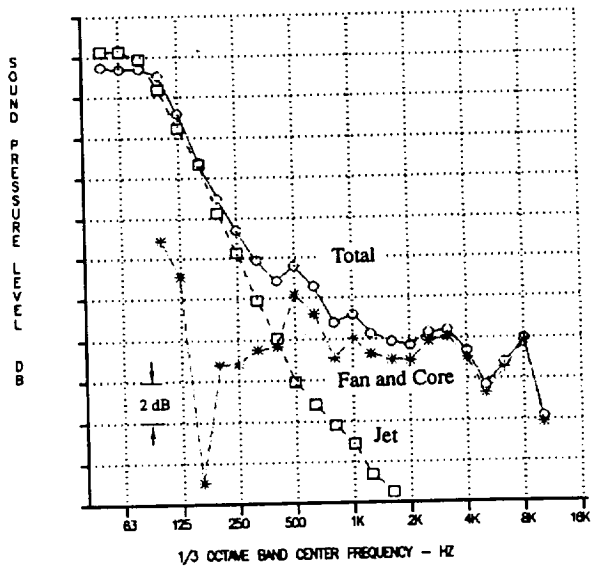

(d) 150 degrees

Figure 20. Spectral Comparisons of the UHBR Jet and the ADP Engine Noise at 89 % Thrust.

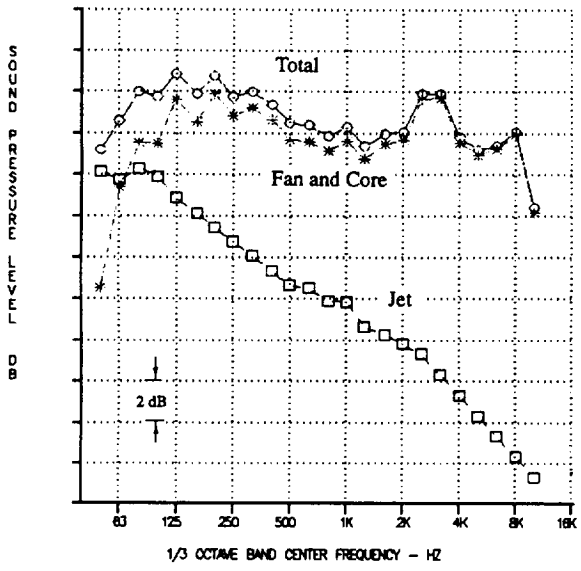

(a) 90 degrees

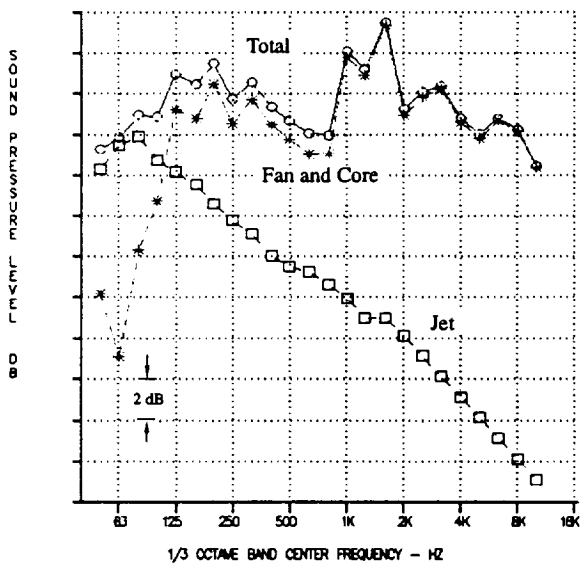

(b) 110 degrees

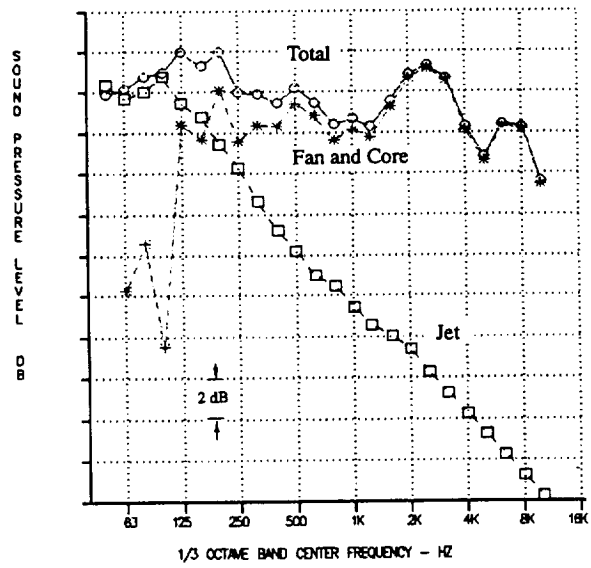

(c) 130 degrees

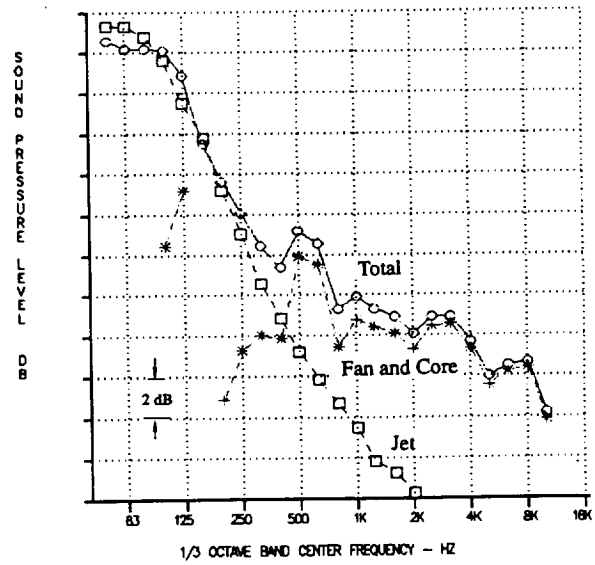

(d) 150 degrees

Figure 21. Spectral Comparisons of the UHBR Jet and the ADP Engine Noise at 92 % Thrust.

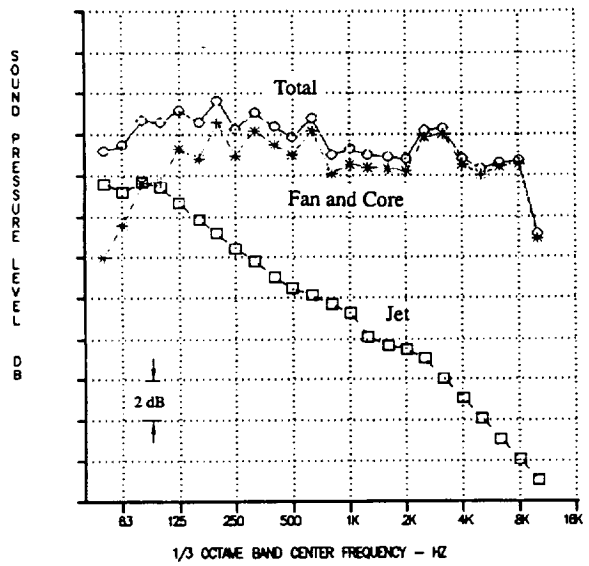

(a) 90 degrees

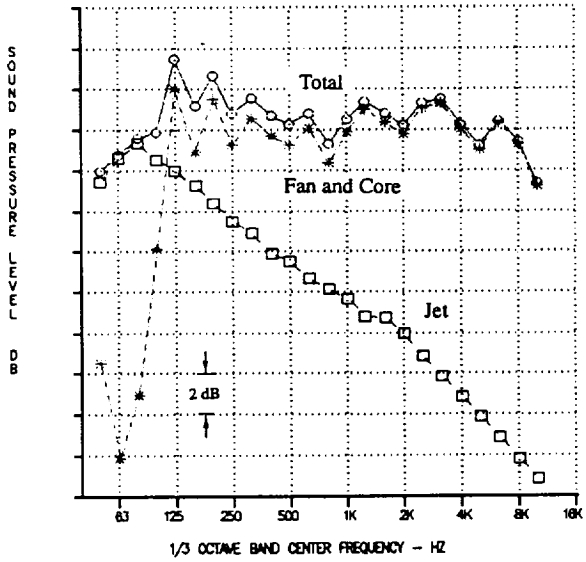

(b) 110 degrees

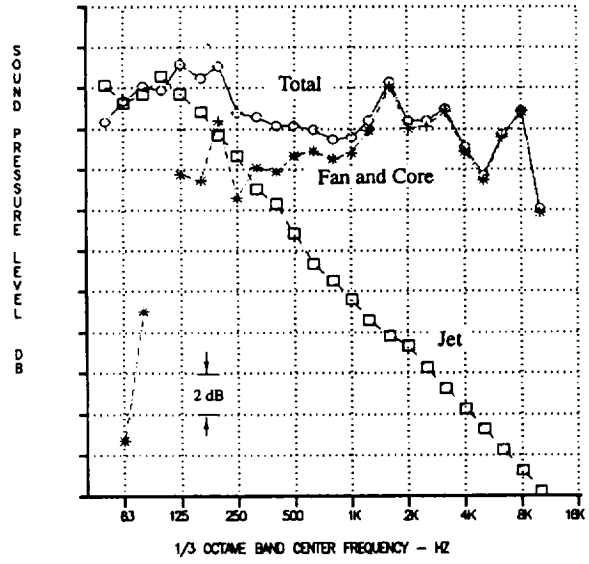

(c) 130 degrees

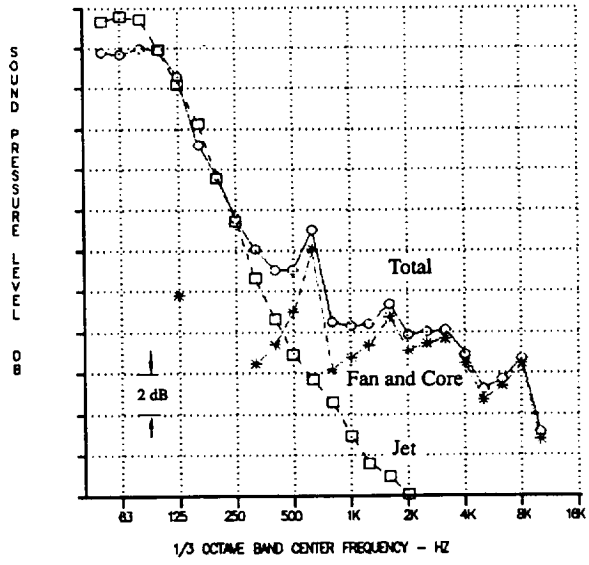

(d) 150 degrees

Figure 22. Spectral Comparisons of the UHBR Jet and the ADP Engine Noise at 100 % Thrust.

5.3 COMPARISON WITH SAE JET NOISE PREDICTIONS

Figures 23 through 29 show comparisons of the Overall Sound Pressure Levels (OASPL) directivities of the jet noise predictions from both the SAE Coaxial Jet and the SAE Single Mixed Flow Jet Noise Prediction Methods (Reference 4) for the seven (7) power settings tested. The SAE Coaxial Jet Noise Method overpredicted the UHBR data by 5 to 6 dB for all seven power settings. The predicted directivity "shapes" are quite consistent with those of the UHBR data. These results suggest that a simple correction of 6 dB to the Coaxial Jet Prediction may be the best interim method to predict the UHBR jet noise. Also shown in the Figures are the jet predictions from the SAE Single Mixed Jet Method. With the exception of the 30% thrust condition shown in Figure 23 where both the SAE Coaxial and Single Mixed Jet predictions were 5 to 6 db higher, the SAE Single Mixed Jet predictions, in general, showed better agreement with the data in terms of absolute levels but not with directivity shapes. The SAE Single Mixed Jet Method overpredicted the UHBR jet at angles less than 130 degrees and underpredicted at the more aft angles.

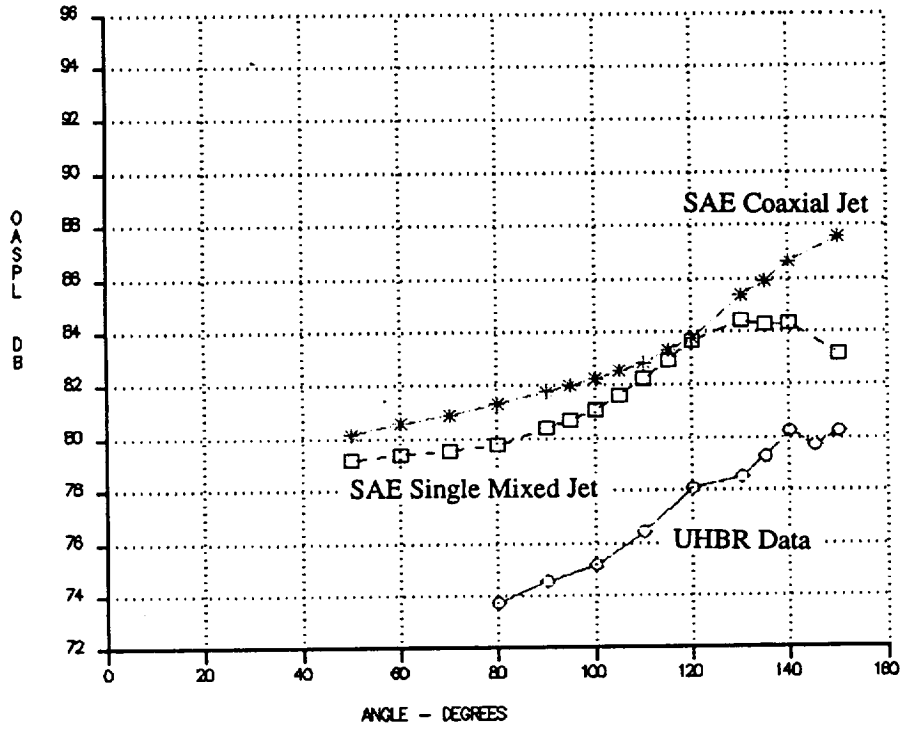

Figure 23. OASPL Directivity Comparison of the SAE Jet Noise Predictions with UHBR Data at 30% Thrust.

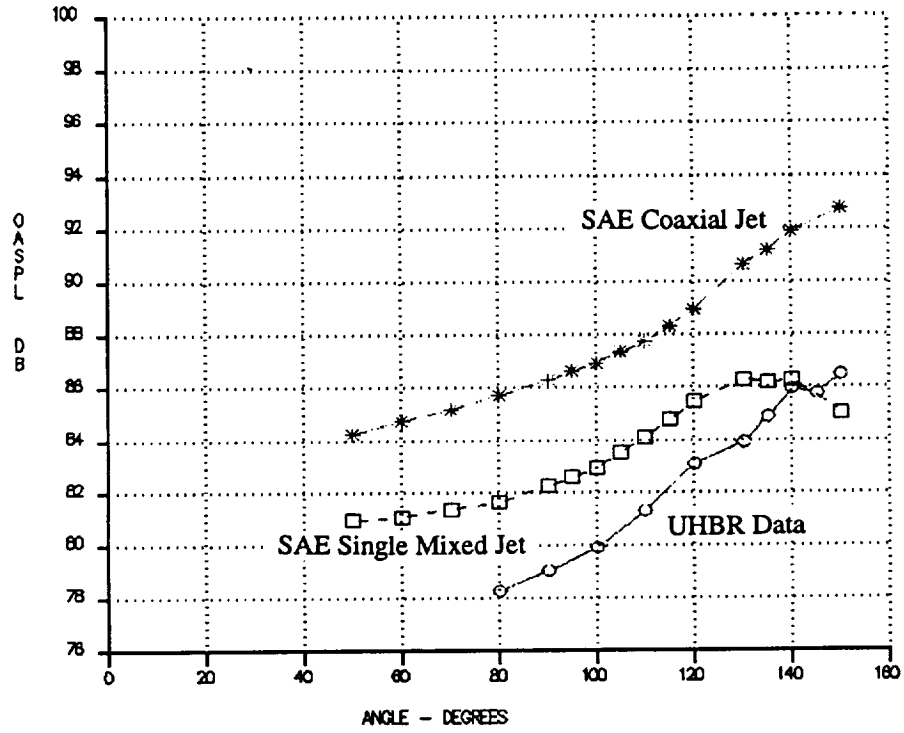

Figure 24. OASPL Directivity Comparison of the SAE Jet Noise Predictions with UHBR Data at 40 % Thrust.

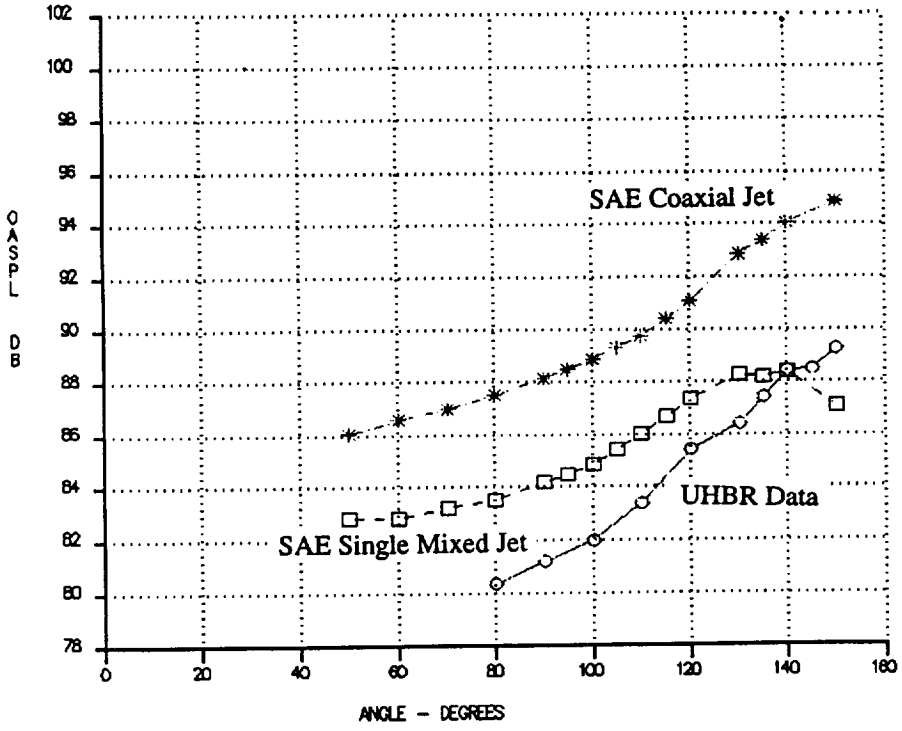

Figure 25. OASPL Directivity Comparison of the SAE Jet Noise Predictions with UHBR Data at 45 % Thrust.

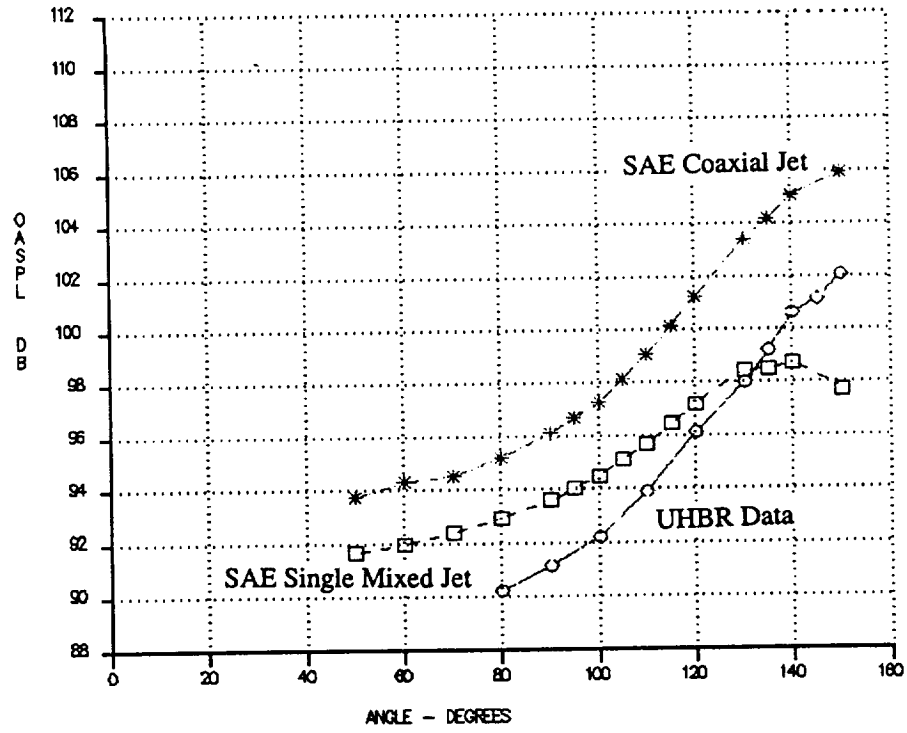

Figure 26. OASPL Directivity Comparison of the SAE Jet Noise Predictions with UHBR Data at 79 % Thrust.

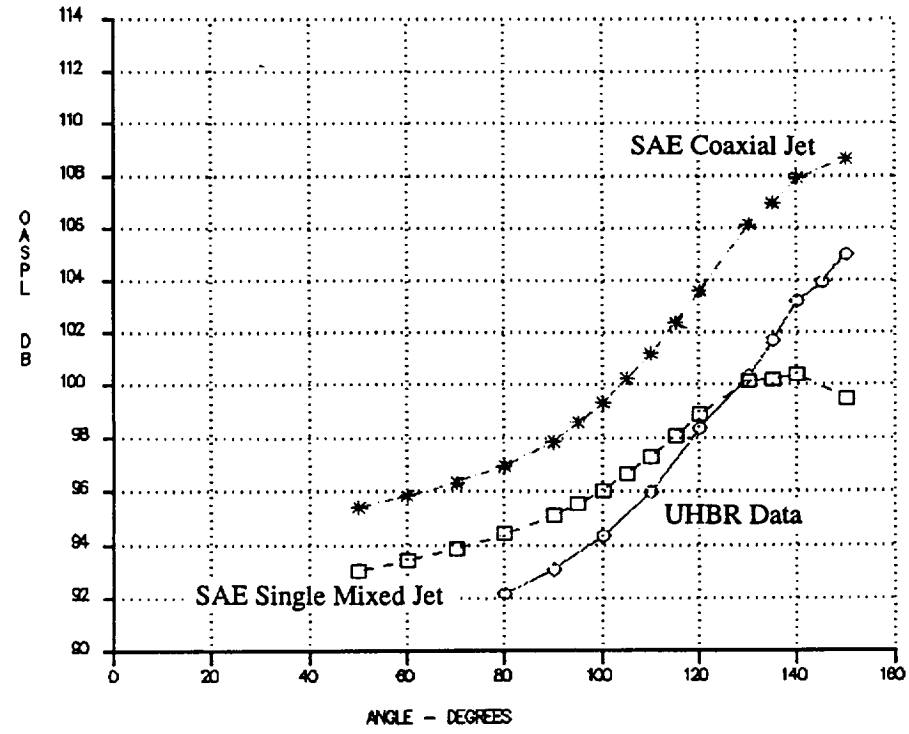

Figure 27. OASPL Directivity Comparison of the SAE Jet Noise Predictions with UHBR Data at 89 % Thrust.

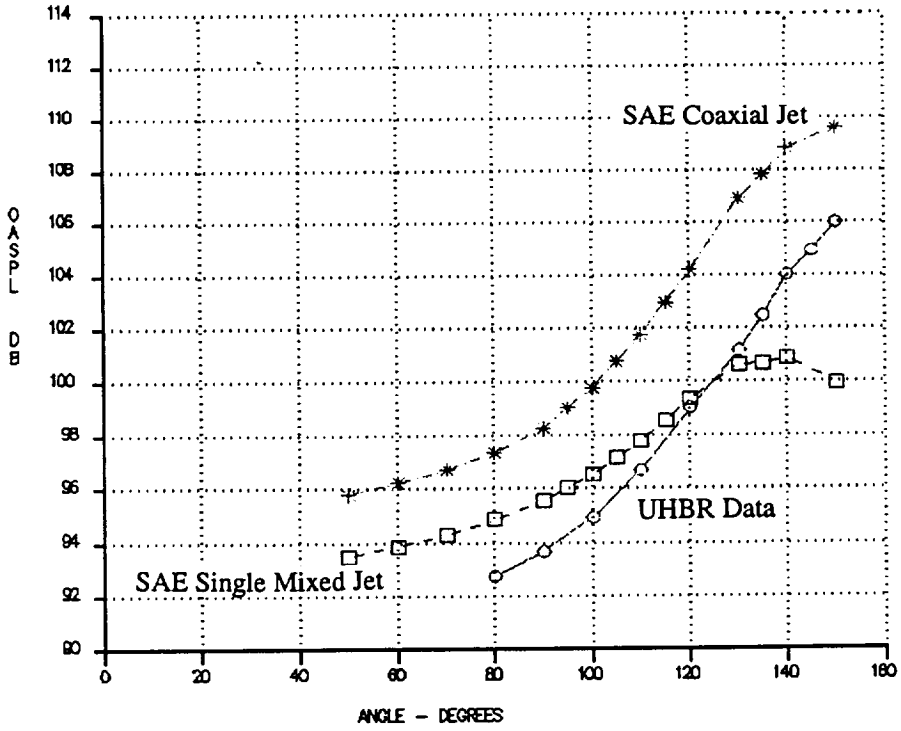

Figure 28. OASPL Directivity Comparison of the SAE Jet Noise Predictions with UHBR Data at 92 % Thrust.

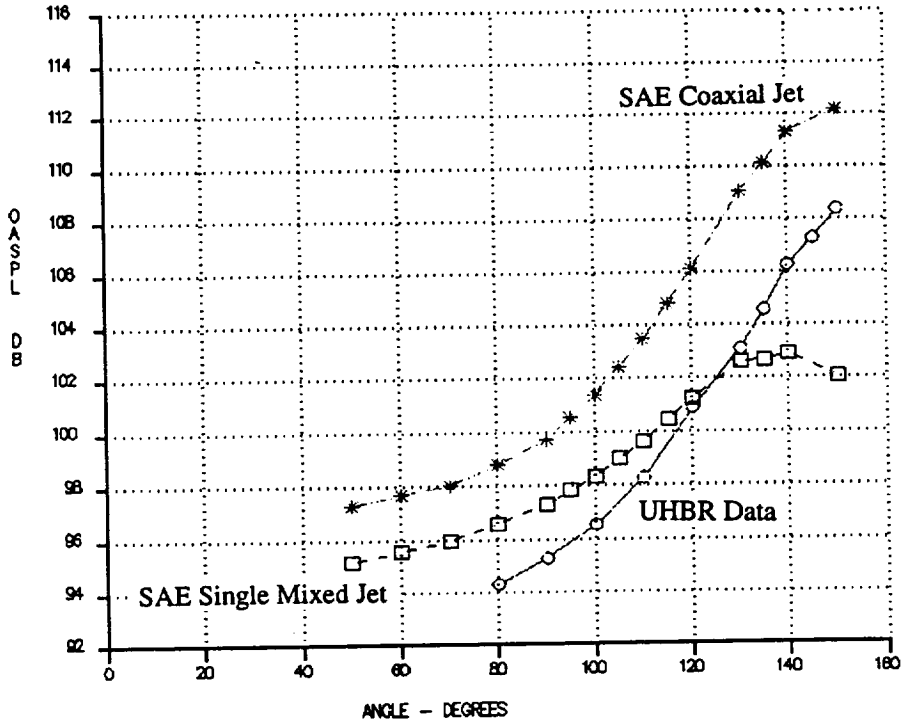

Figure 29. OASPL Directivity Comparison of the SAE Jet Noise Predictions with UHBR Data at 100 % Thrust.

Spectral comparisons of the SAE jet predictions with the UHBR data are shown in Figures 30 through 36 for all seven (7) power settings.

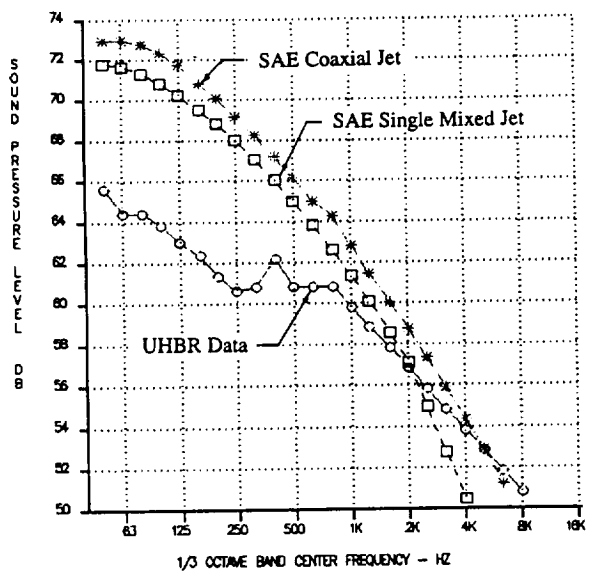

(a) 90 degrees

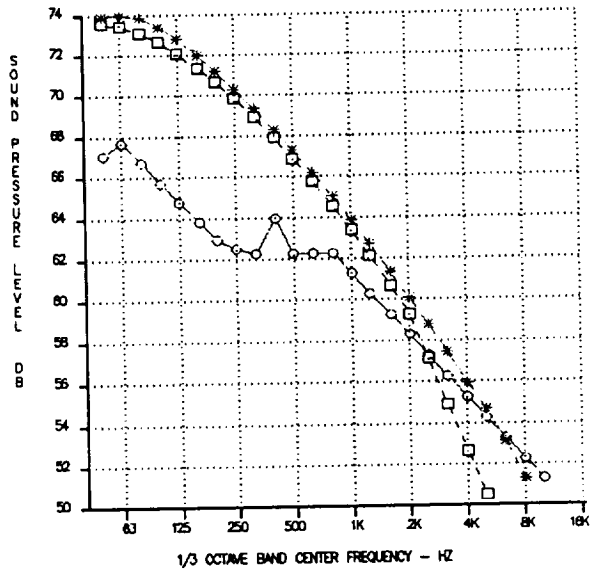

(b) 110 degrees

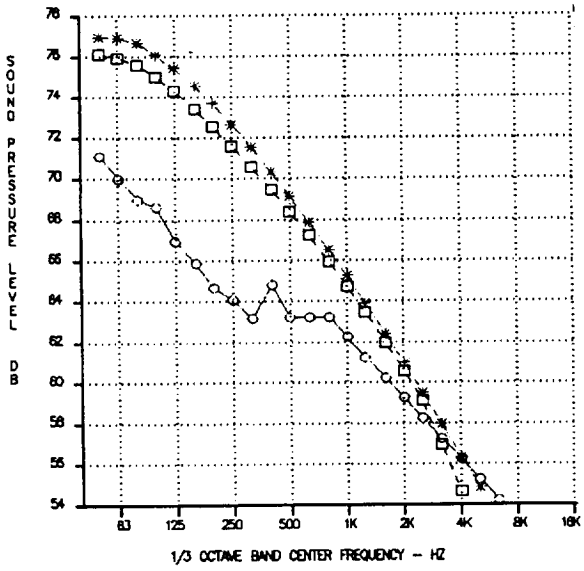

(c) 130 degrees

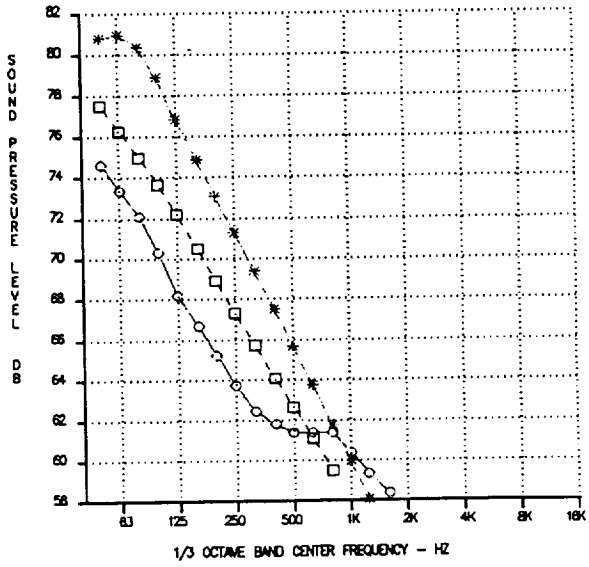

(d) 150 degrees

Figure 30. SPL Spectral Comparisons of the SAE Jet Noise Predictions with UHBR Data at 30 % Thrust.

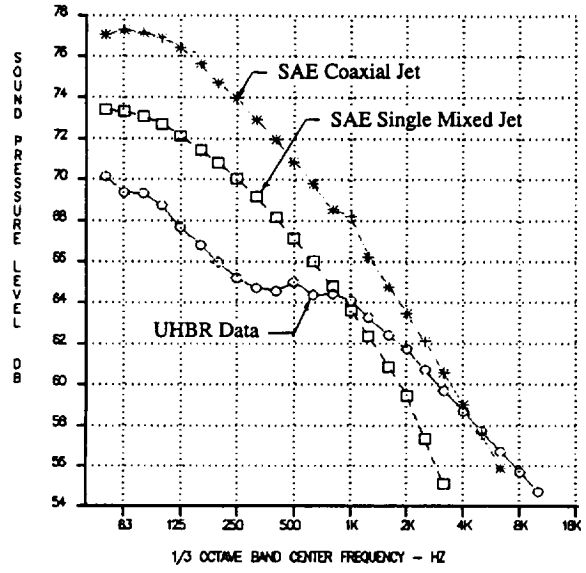

(a) 90 degrees

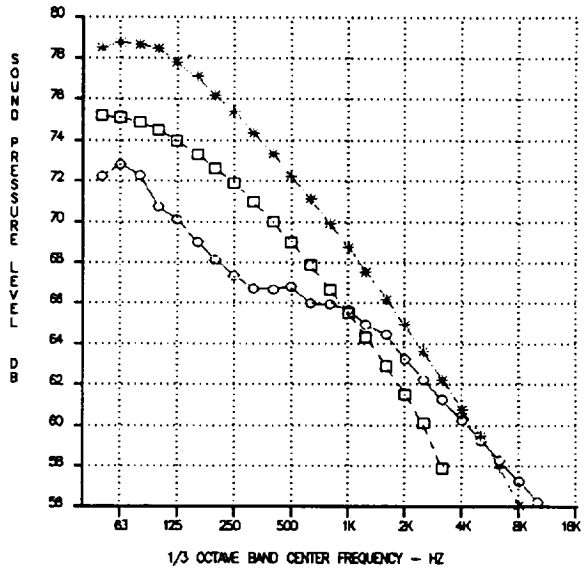

(b) 110 degrees

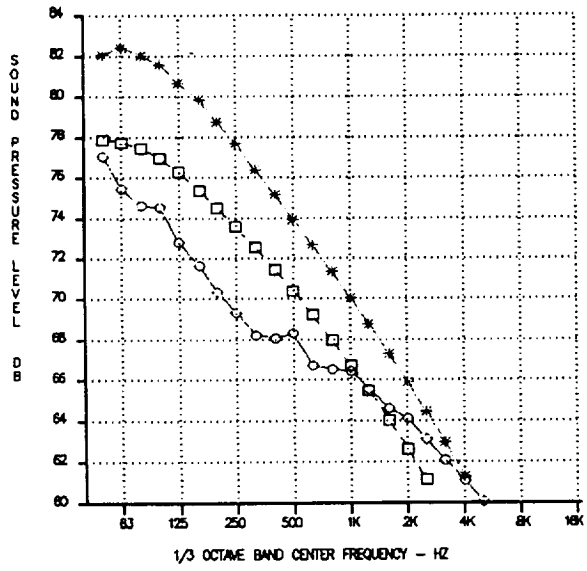

(c) 130 degrees

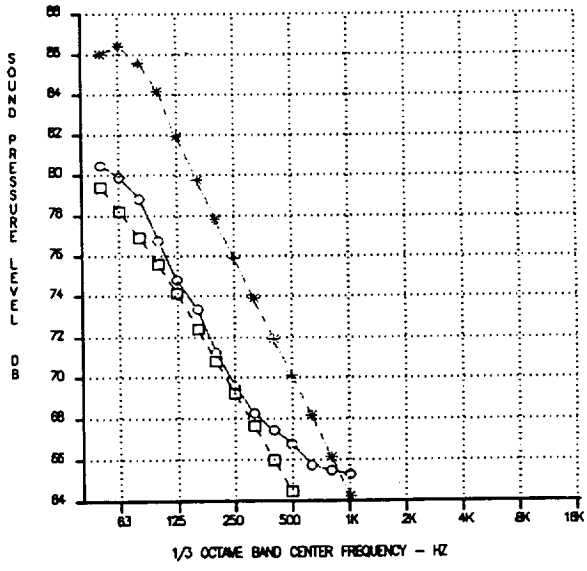

(d) 150 degrees

Figure 31. SPL Spectral Comparisons of the SAE Jet Noise Predictions with UHBR Data at 40 % Thrust.

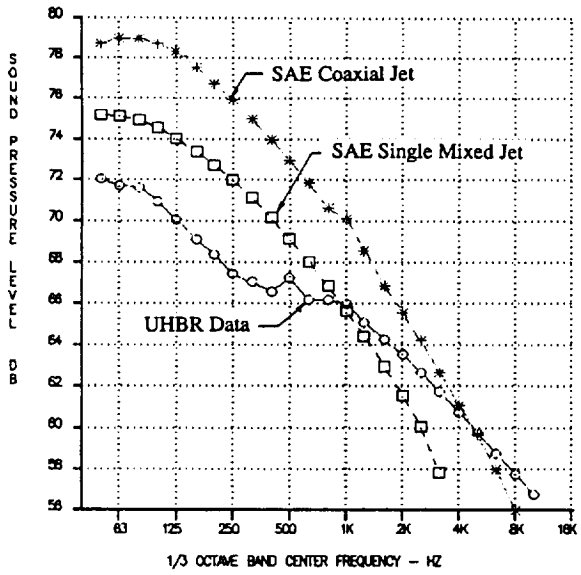

(a) 90 degrees

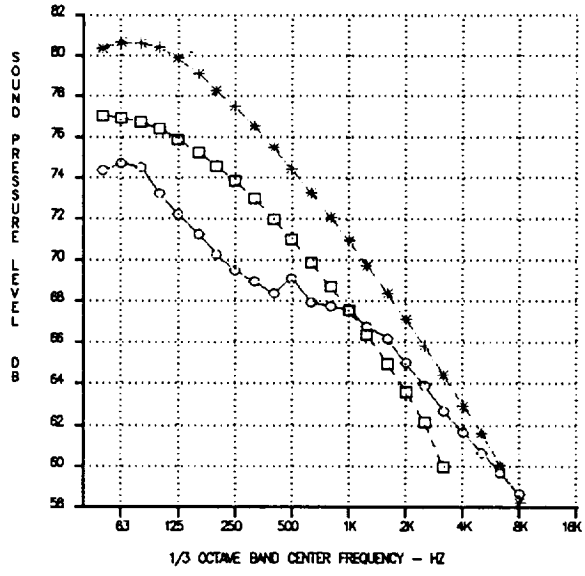

(b) 110 degrees

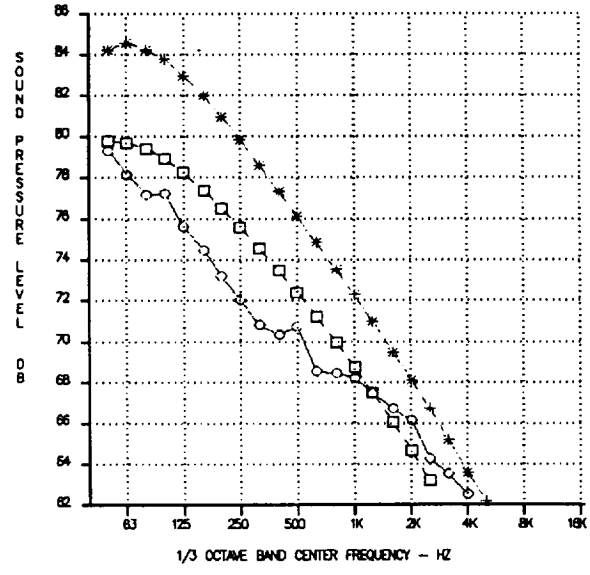

(c) 130 degrees

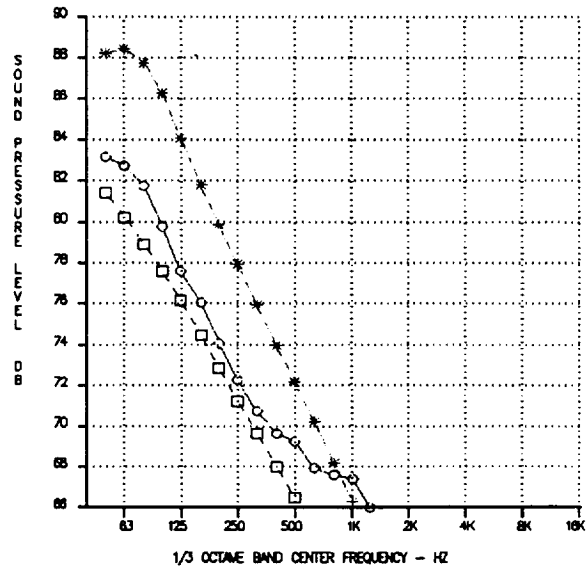

(d) 150 degrees

Figure 32. SPL Spectral Comparisons of the SAE Jet Noise Predcictions with UHBR Data at 45 % Thrust.

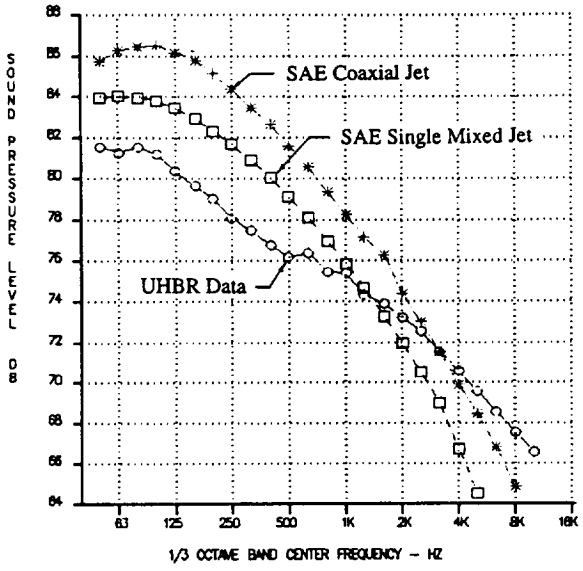

(a) 90 degrees

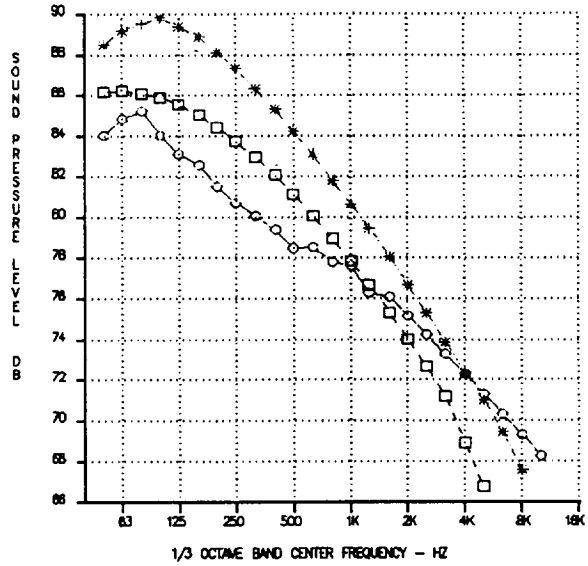

(b) 110 degrees

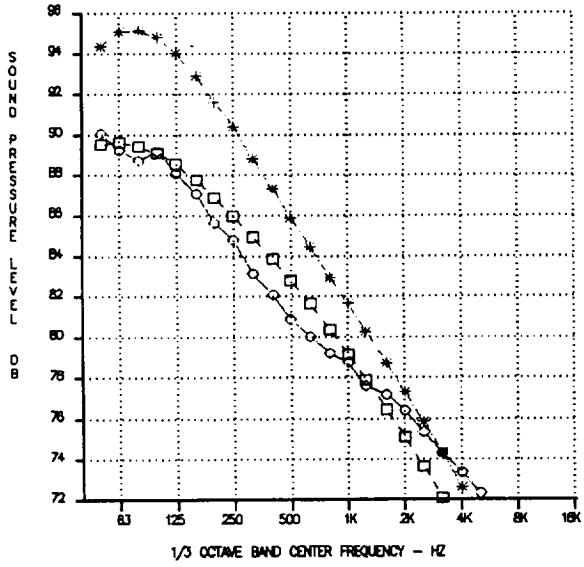

(c) 130 degrees

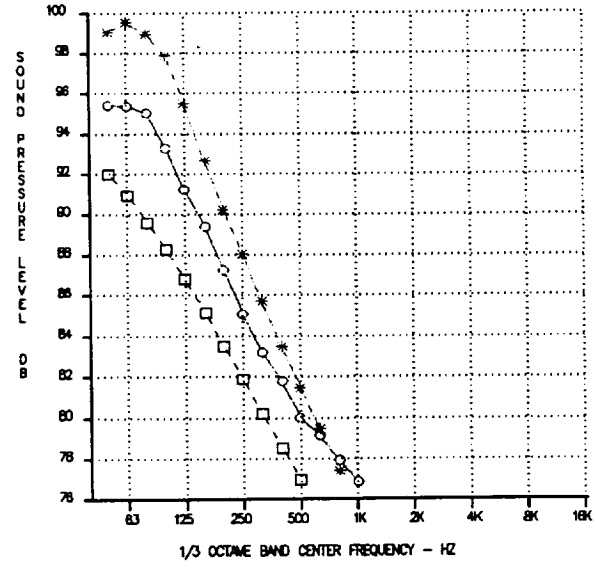

(d) 150 degrees

Figure 33. SPL Spectral Comparisons of the SAE Jet Noise Predictions with UHBR Data at 79 % Thrust

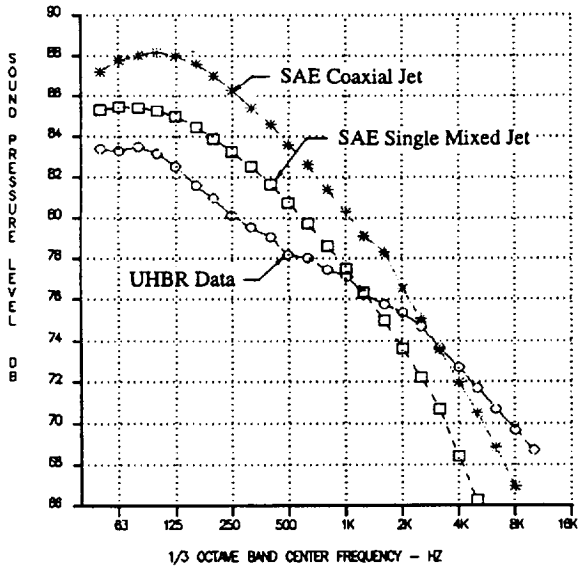

(a) 90 degrees

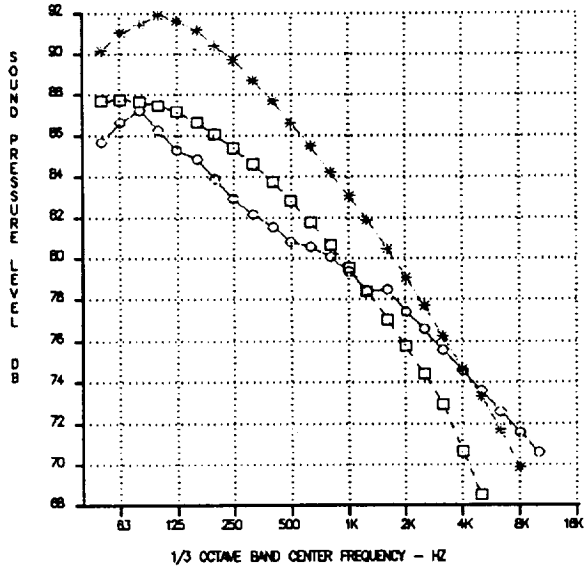

(b) 110 degrees

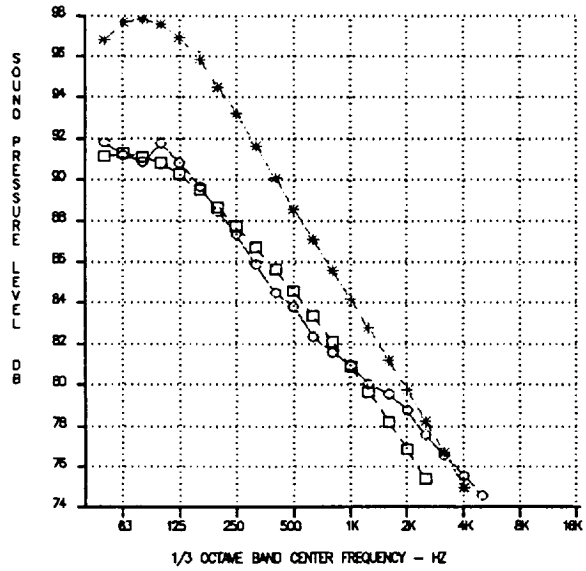

(c) 130 degrees

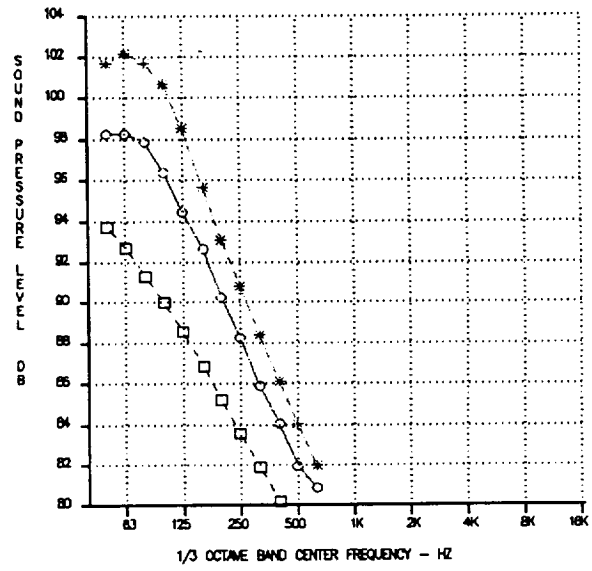

(d) 150 degrees

Figure 34. SPL Spectral Comparisons of the SAE Jet Noise Predictions with UHBR Data at 89 % Thrust

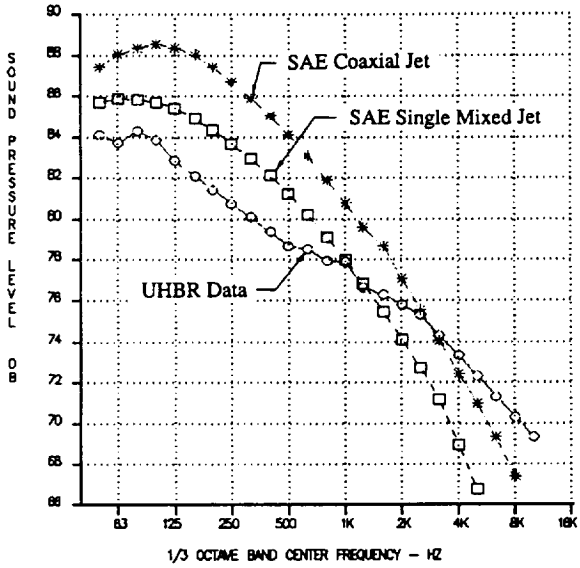

(a) 90 degrees

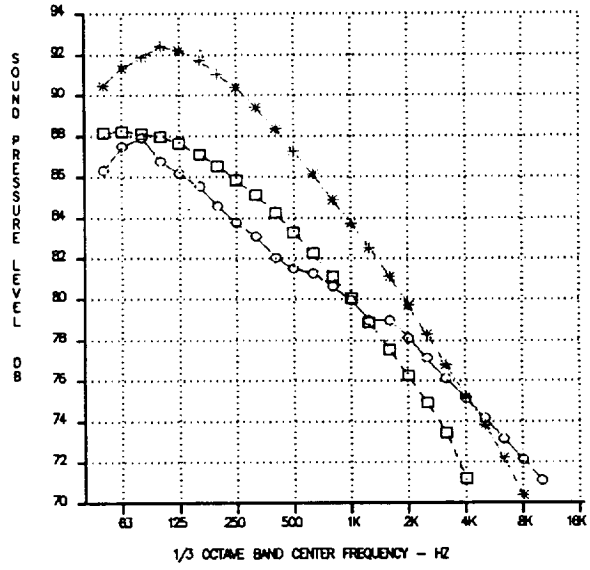

(b) 110 degrees

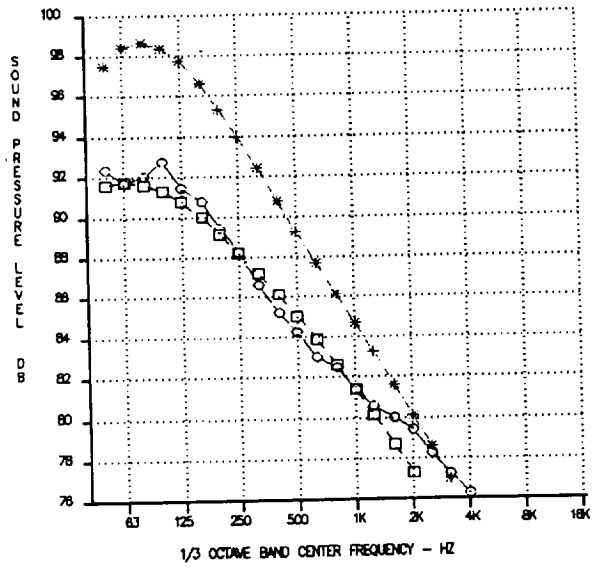

(c) 130 degrees

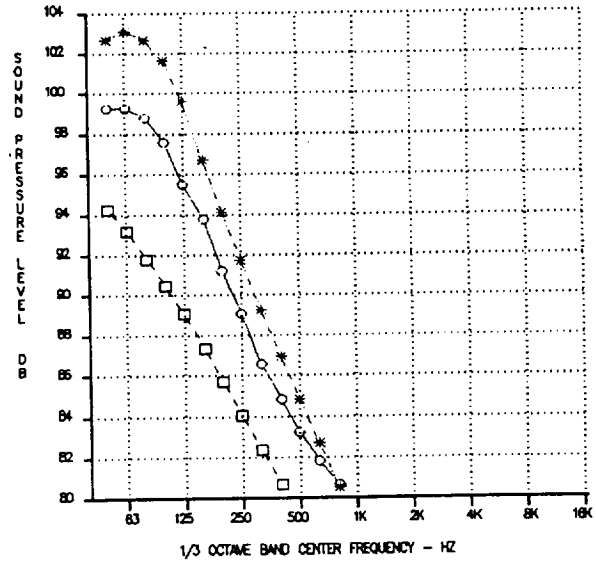

(d) 150 degrees

Figure 35. SPL Spectral Comparisons of the SAE Jet Noise Predictions with UHBR Data at 92 % Thrust

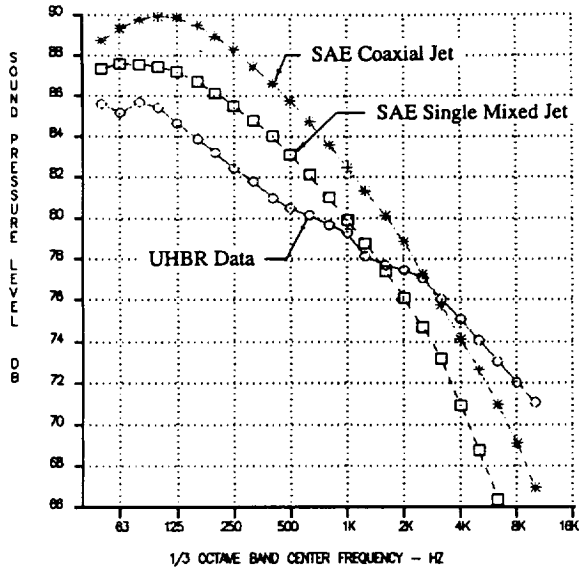

(a) 90 degrees

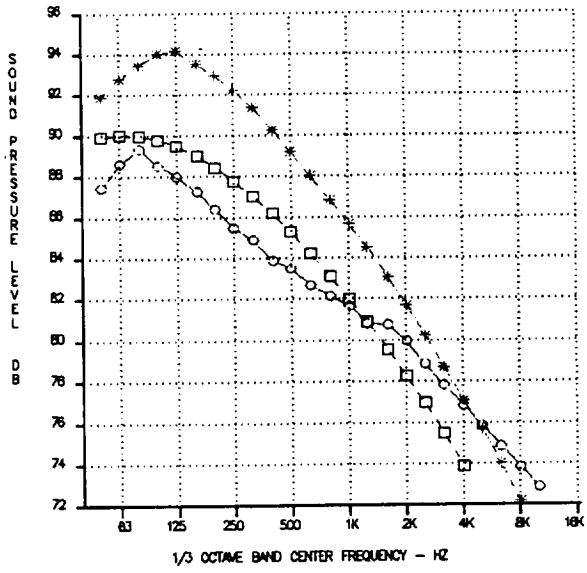

(b) 110 degrees

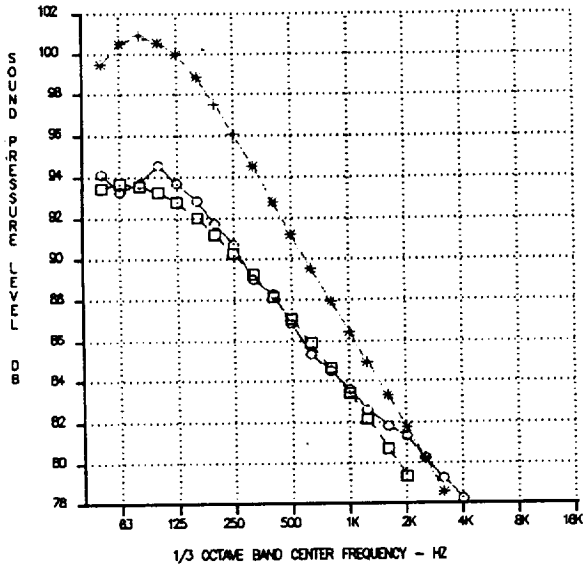

(c) 130 degrees

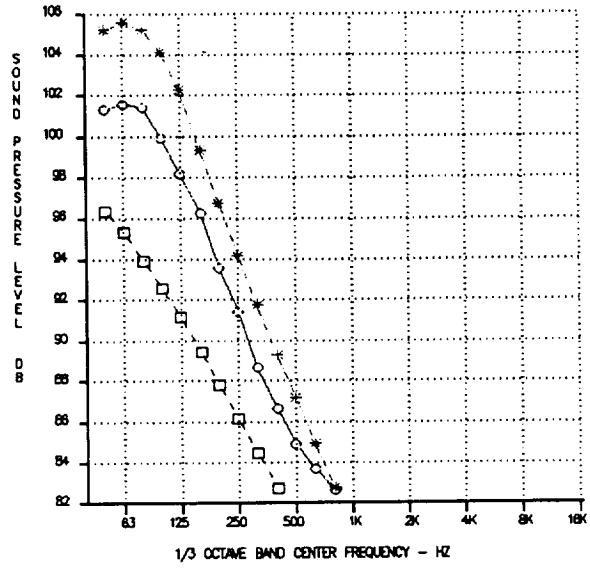

(d) 150 degrees

Figure 36. SPL Spectral Comparisons of the SAE Jet Noise Predictions with UHBR Data at 100 % Thrust

For the coaxial jet, it is generally assumed there are three source noise components from the primary, the secondary and the merged jet. The primary jet component dominates the high frequency, the secondary jet component the mid frequency and the merged jet the low frequency portion of the predicted coaxial jet noise spectra. The comparisons indicated that the 5 to 6 dB overpredictions of the SAE Coaxial Jet Method are primarily on the low–frequency "merged jet" portions of the noise spectra. Thus a simple 6 dB correction to the predicted "merged jet" portion of the SAE Coaxial Jet Method would be the best interim method of predicting the UHBR jet noise. The SAE Single Mixed Jet Method tends to overpredict the low–frequency and underpredict the high–frequency portion of the spectra (with the exception of the excellent agreement at 130 degrees). For these reasons, the SAE Single Mixed Jet Method is not recommended for the prediction of the UHBR jet noise.

5.4 FLIGHT EFFECTS ON UHBR JET NOISE SPECTRA

Figures 37 through 40 show the effects of the wind tunnel Mach number on the UHBR jet noise SPL spectra at four (4) of the seven (7) power settings tested (79%, 89%, 92% and 100% thrust). The flight noise reductions are consistent across the entire UHBR broad jet noise spectra and are not confined only to the low–frequency portions of the spectra as often the case with "mixer" type nozzles. These results suggest that the forward flight effect affects the merged, the secondary as well as the primary jet source component in the coaxial nozzle jet.

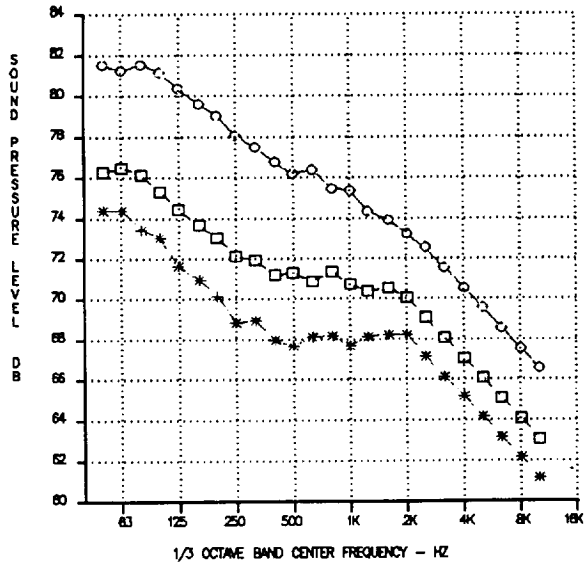

(a) 90 degrees

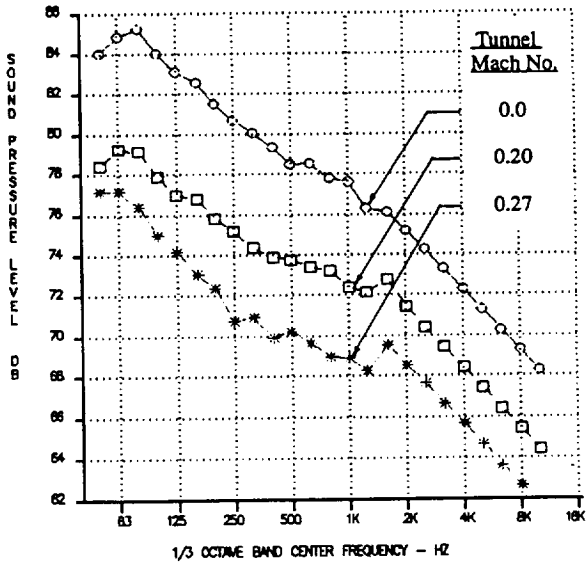

(b) 110 degrees

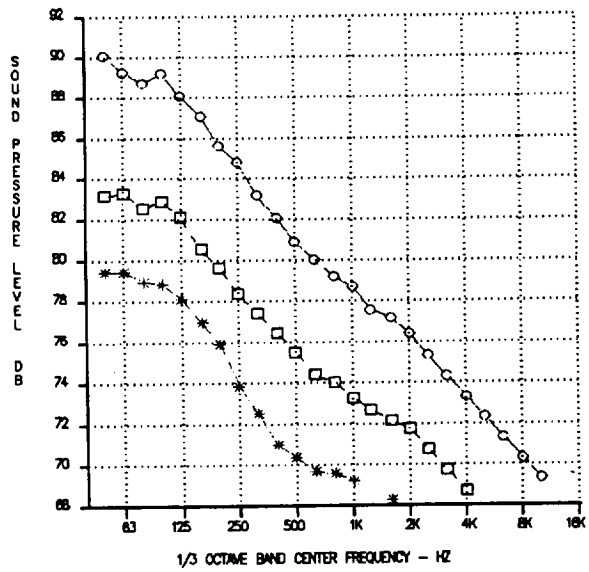

(c) 130 degrees

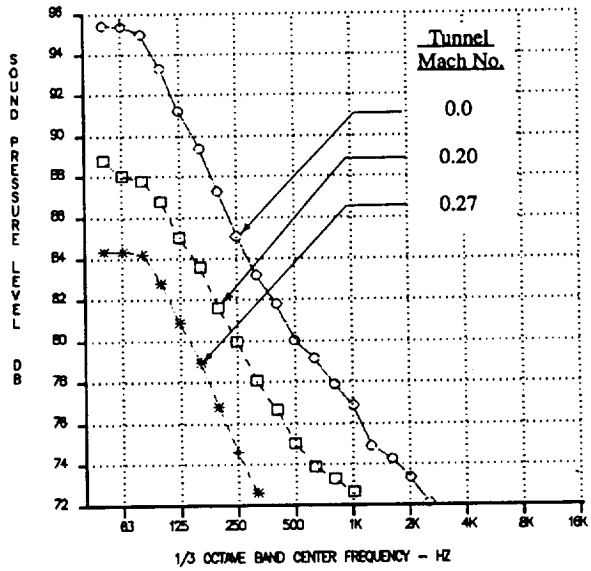

(d) 150 degrees

Figure 37. Effects of Forward Flight Mach Number on UHBR Jet Noise Spectra at 79 % Thrust.

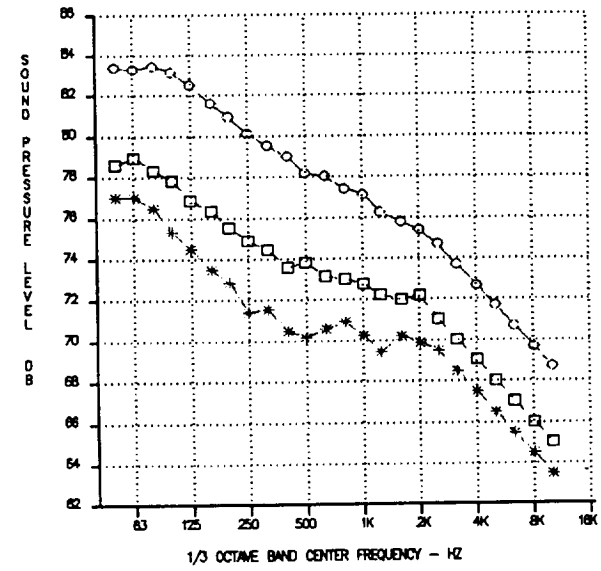

(a) 90 degrees

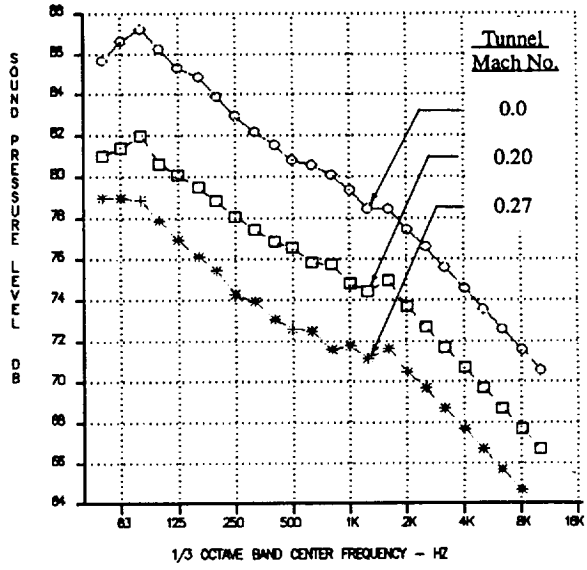

(b) 110 degrees

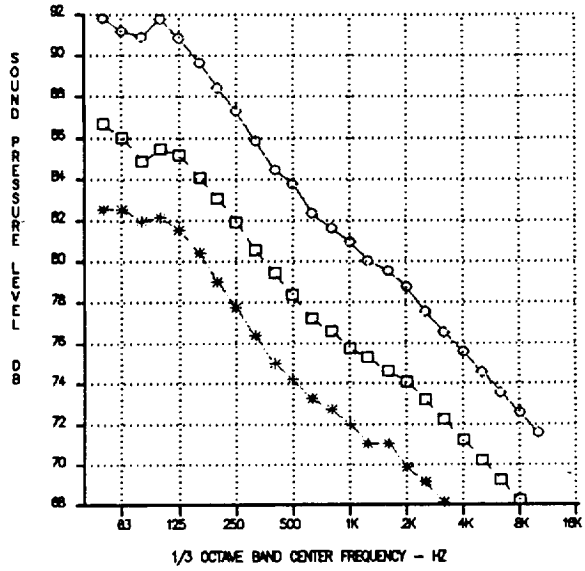

(c) 130 degrees

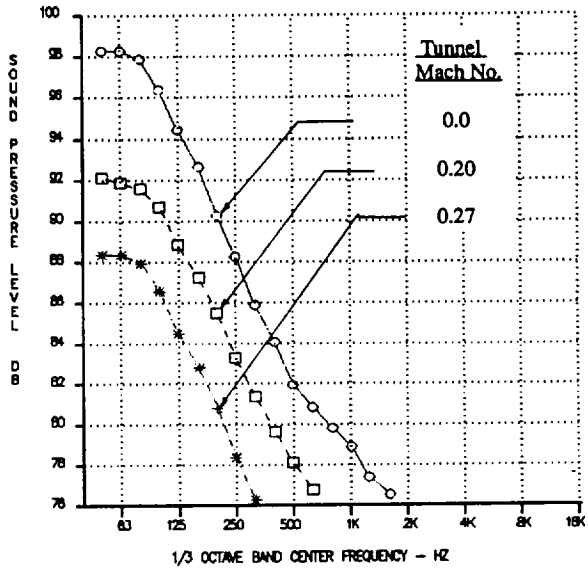

(d) 150 degrees

Figure 38. Effects of Forward Flight Mach Number on UHBR Jet Noise Spectra at 89 % Thrust.

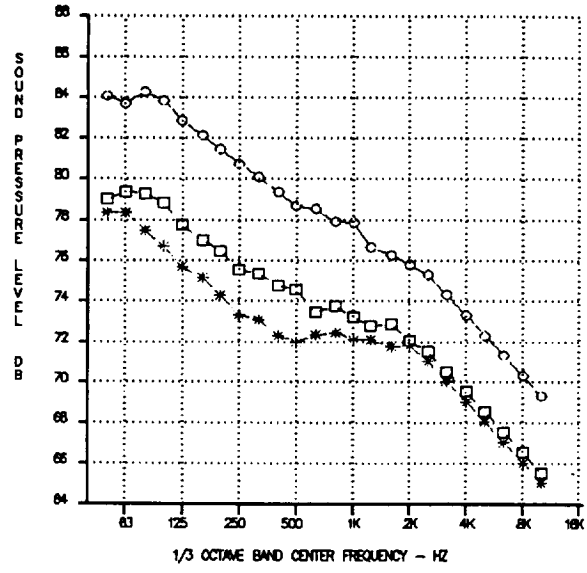

(a) 90 degrees

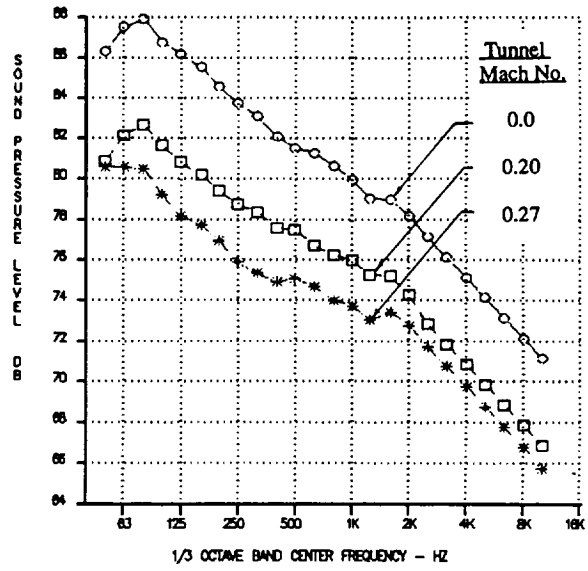

(b) 110 degrees

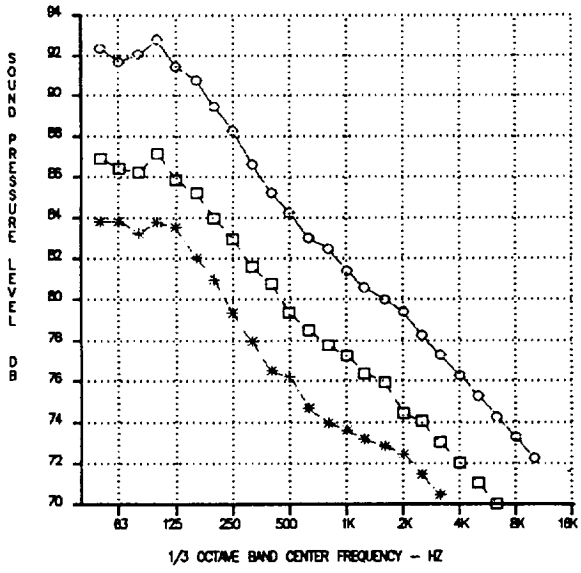

(c) 130 degrees

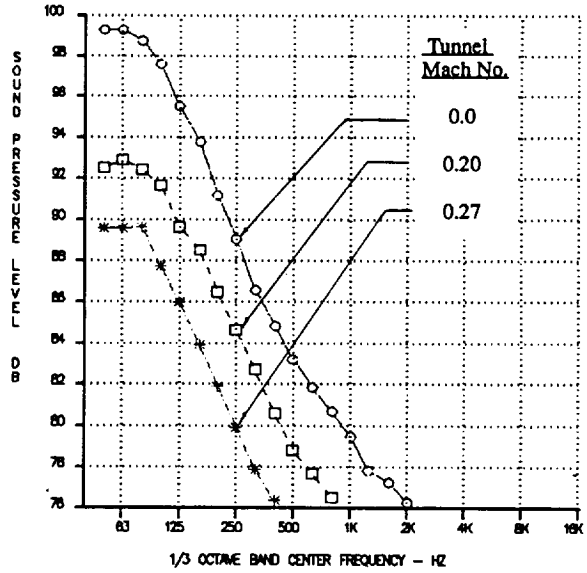

(d) 150 degrees

Figure 39. Effects of Forward Flight Mach Number on UHBR Jet Noise Spectra at 92 % Thrust.

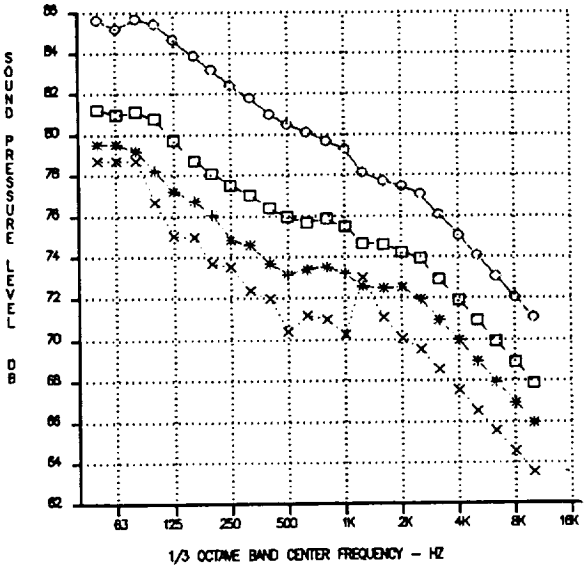

(a) 90 degrees

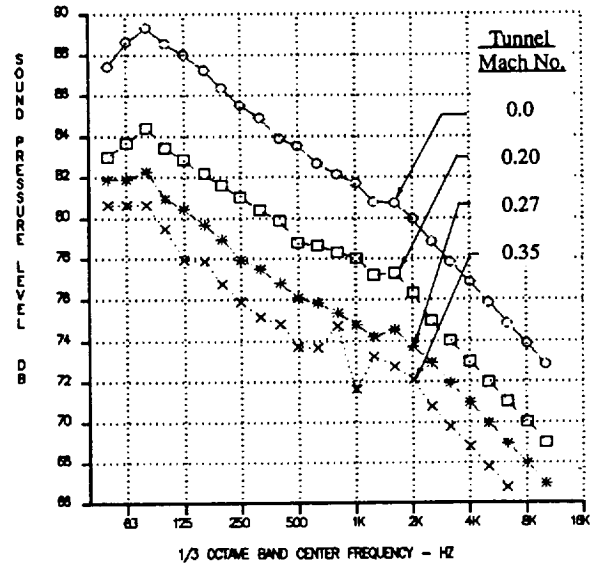

(d) 110 degrees

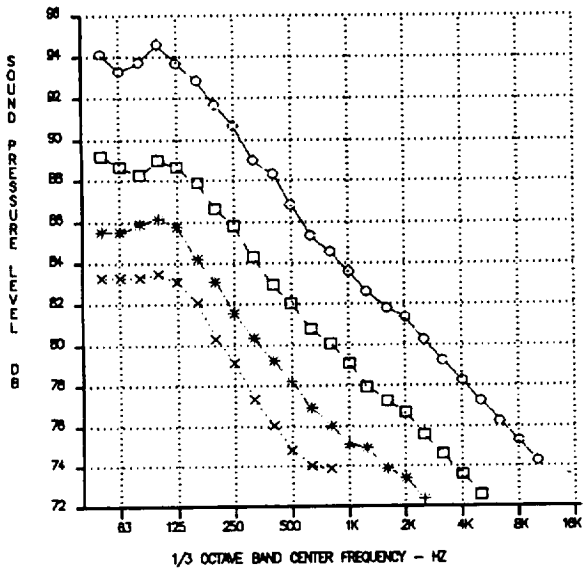

(c) 130 degrees

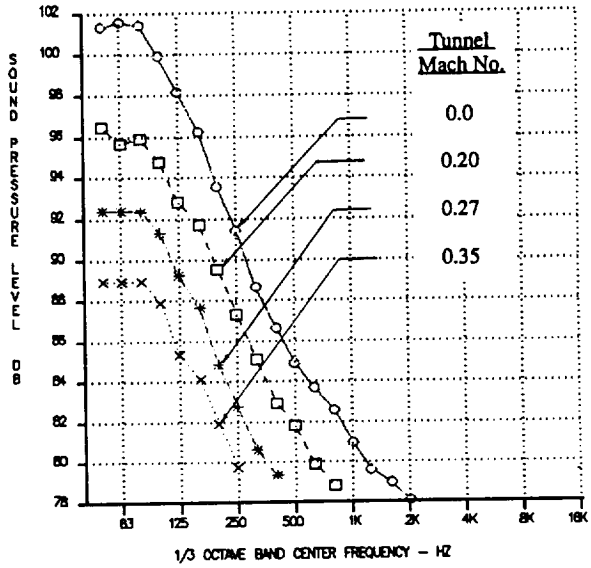

(d) 150 degrees

Figure 40. Effects of Forward Flight Mach Number on UHBR Jet Noise Spectra at 100 % Thrust.

The jet OASPL directivities corresponding to the UHBR jet noise spectra presented in the above Figures are shown in Figures 41 to 44 respectively.

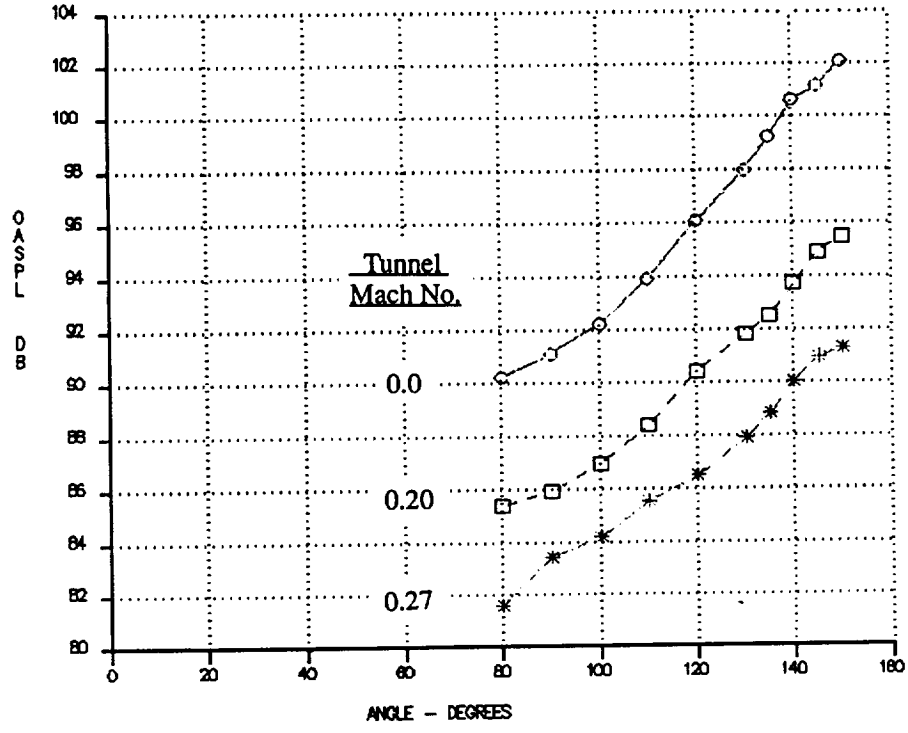

Figure 41. Effect of Flight Mach Number on UHBR Jet OASPL Directivities at 79 % Thrust.

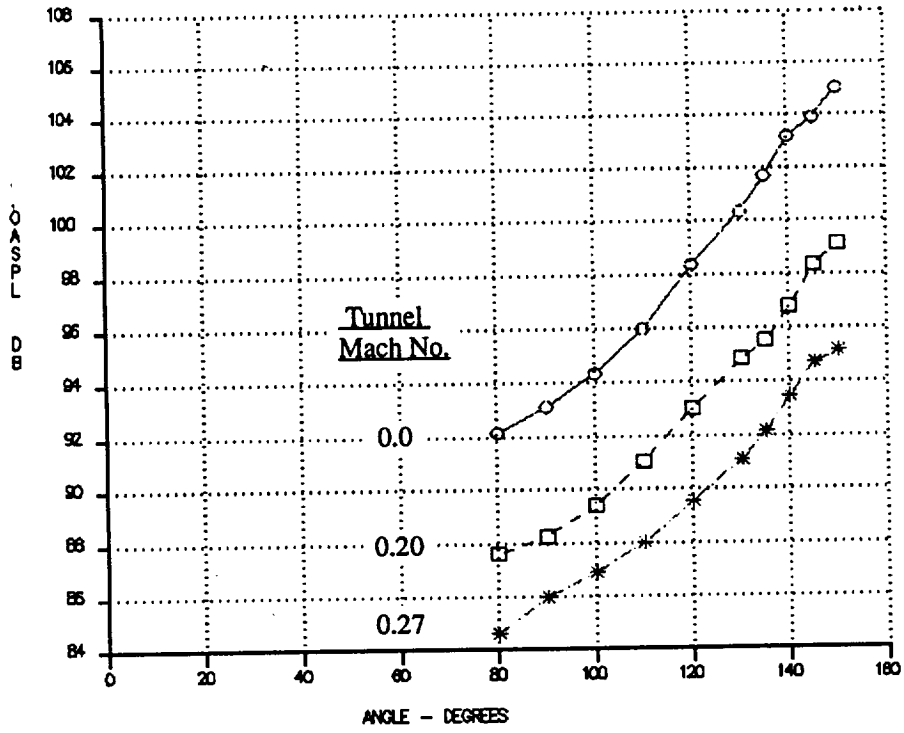

Figure 42. Effect of Flight Mach Number on UHBR Jet OASPL Directivities at 89 % Thrust

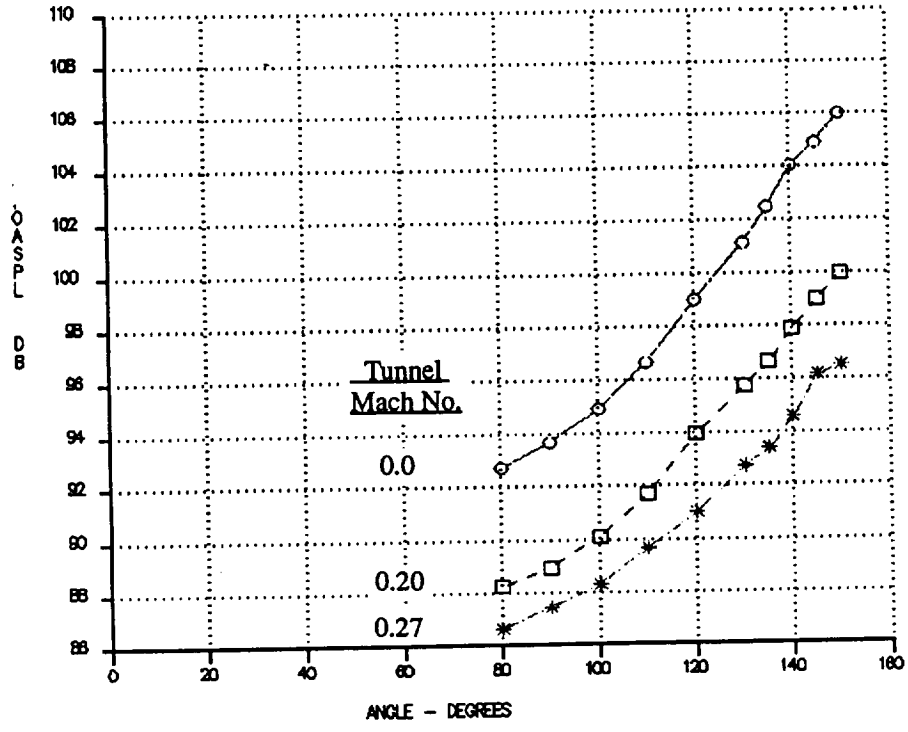

Figure 43. Effect of Flight Mach Number on UHBR Jet OASPL Directivities at 92 % Thrust.

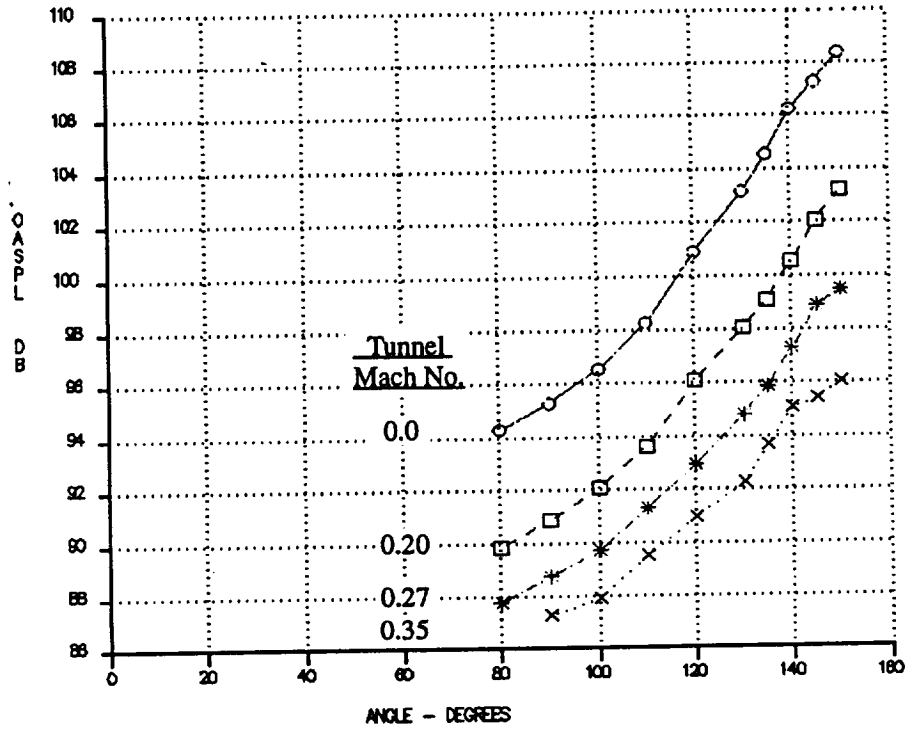

Figure 44. Effect of Flight Mach Number on UHBR Jet OASPL Directivities at 100 % Thrust

These jet OASPL reductions from forward flight can be correlated with a relative jet velocity parameter (10 log [(Vp – Vt) / (Vp)]) where Vp is the primary jet velocity (is also V_{pri}), and Vt is the wind tunnel/forward flight speed. For the wind tunnel Mach numbers tested, the average tunnel temperature is 35 deg. F. The flight speeds for Mach numbers 0.20, 0.27 and 0.35 are 219, 295 and 382 ft/sec. These jet OASPL reductions versus relative velocities correlations and the resultant slopes of these correlations (also known as jet noise relative velocity exponents) are presented in Section 5.5

5.5 CORRELATION OF JET OASPL NOISE REDUCTIONS WITH RELATIVE JET VELOCITY (FLIGHT EXPONENTS)

The jet OASPL reductions versus the relative jet velocity parameter (10 log [(Vp – Vt) / (Vp)]) correlations are shown in Figures 45 through 54 for angles 80 through 150 degrees, respectively. (Vp and Vt are the primary jet velocity and wind tunnel velocity, respectively). The slopes of these correlations are known as jet noise relative velocity exponents. These exponents varied from 5.17 at 90 degrees to 9.58 at 150 degrees. A summary of the values of these exponents is given in Table 3. With the exceptions of the 80– and 130–degrees angles, the exponents increased with increasing angles. These relative velocity exponents should be applied to all source components for the coaxial jet when predicting inflight noise levels of the coaxial jet.

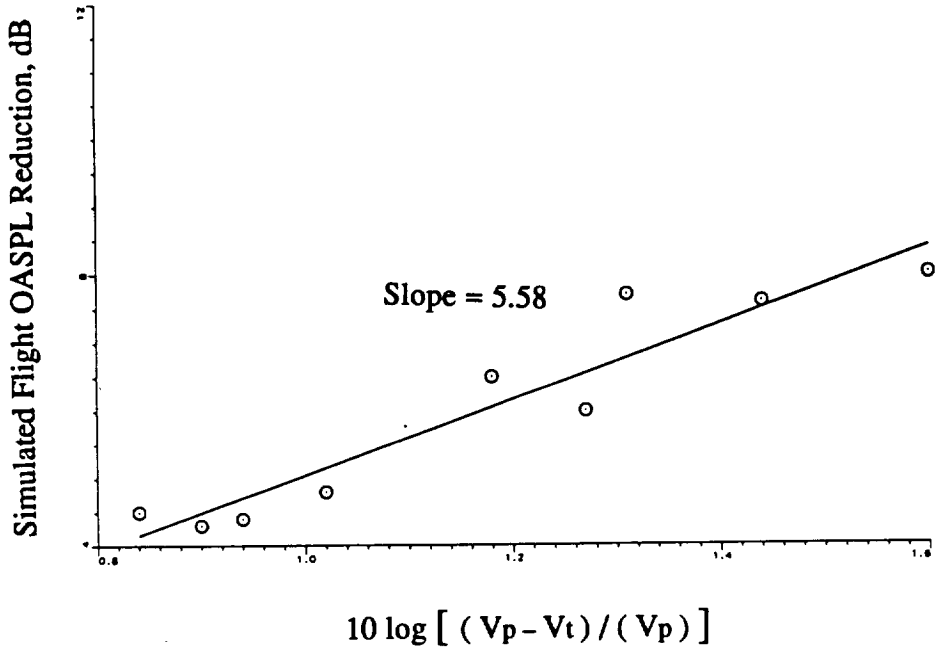

Figure 45. Correlations of Jet Noise OASPL Reductions with the Relative Jet Velocity Parameter for 80–degrees Angle.

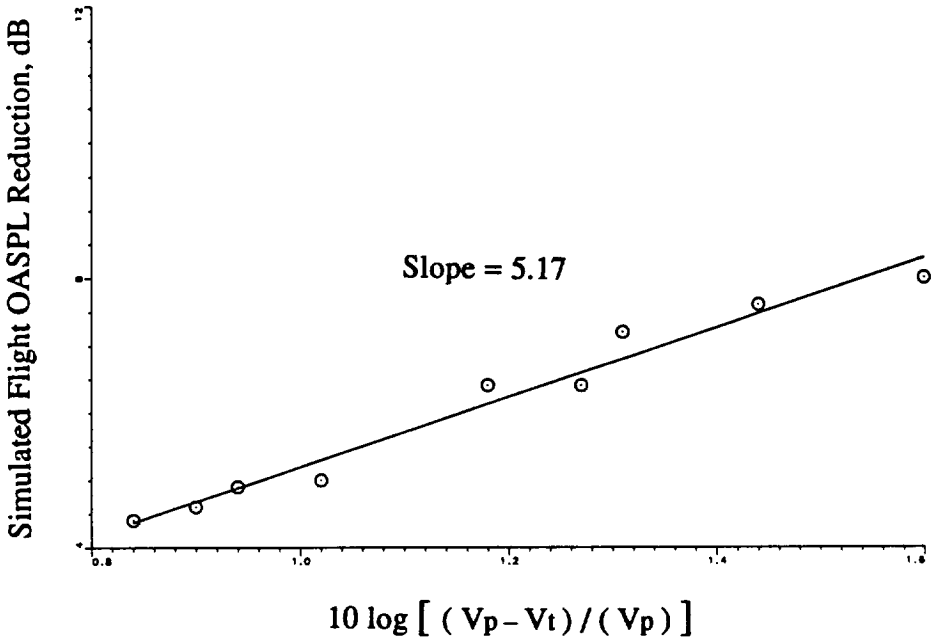

Figure 46. Correlations of Jet Noise OASPL Reductions with the Relative Jet Velocity Parameter for 90–degrees Angle.

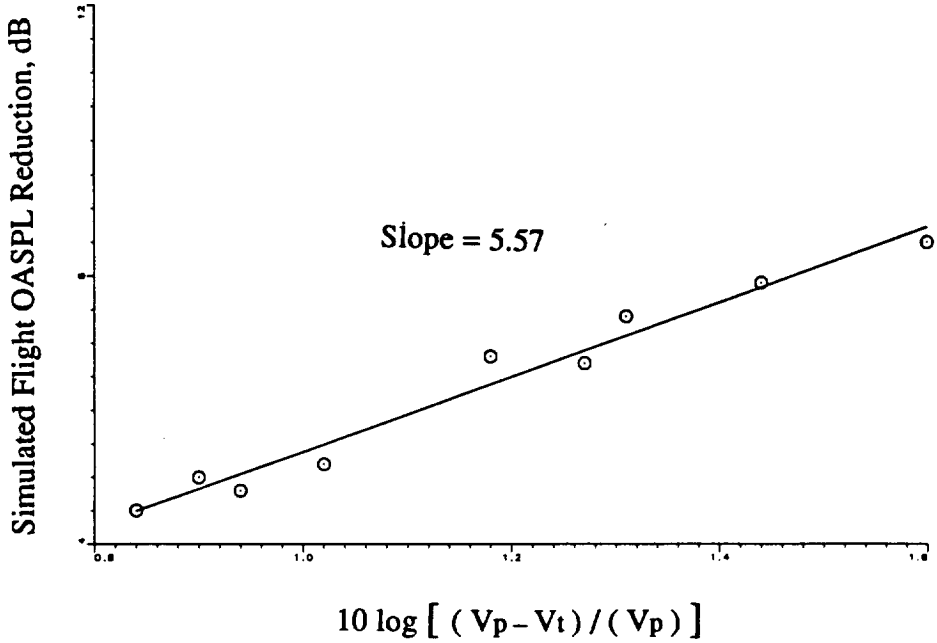

Figure 47. Correlations of Jet Noise OASPL Reductions with the Relative Jet Velocity Parameter for 100–degrees Angle.

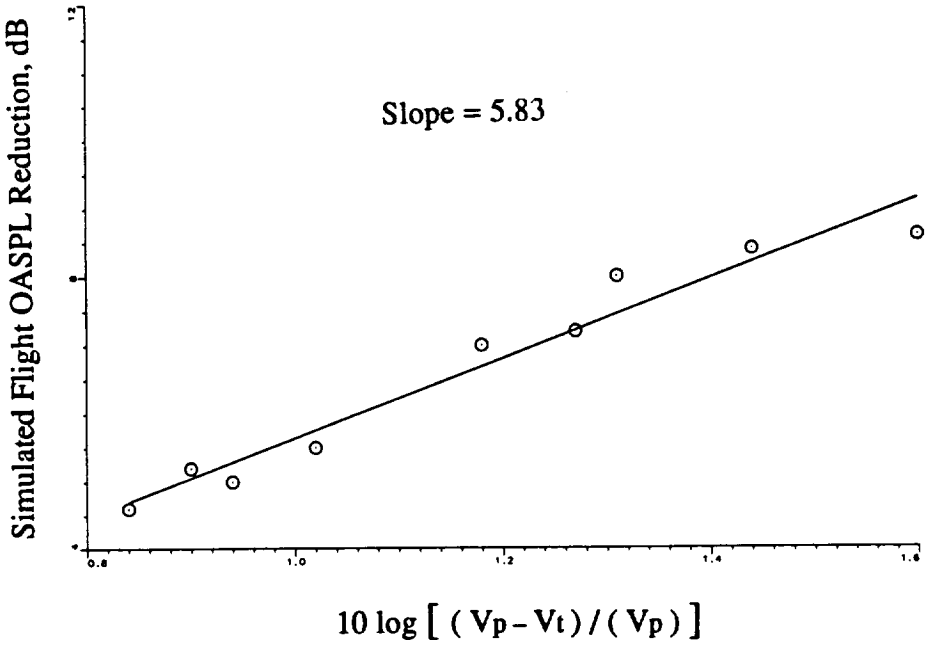

Figure 48. Correlations of Jet Noise OASPL Reductions with the Relative Jet Velocity Parameter for 110–degrees Angle.

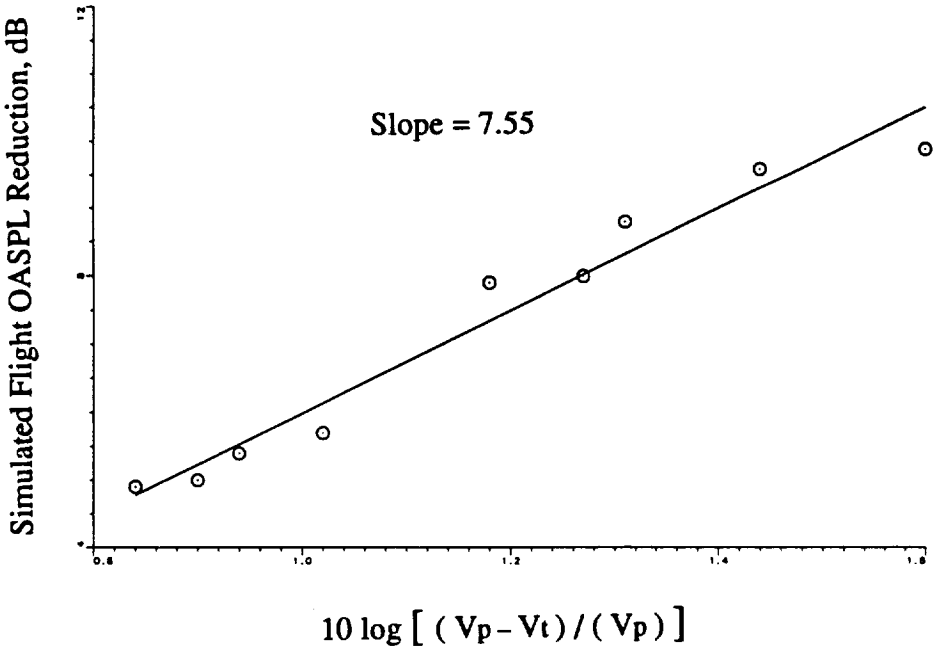

Figure 49. Correlations of Jet Noise OASPL Reductions with the Relative Jet Velocity Parameter for 120–degrees Angle.

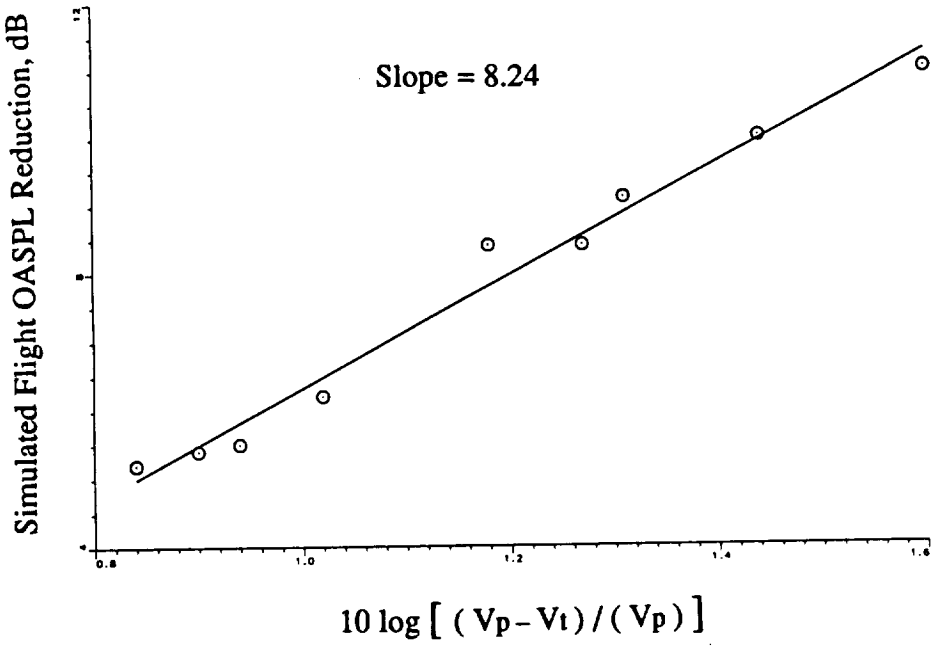

Figure 50. Correlations of Jet Noise OASPL Reductions with the Relative Jet Velocity Parameter for 130–degrees Angle.

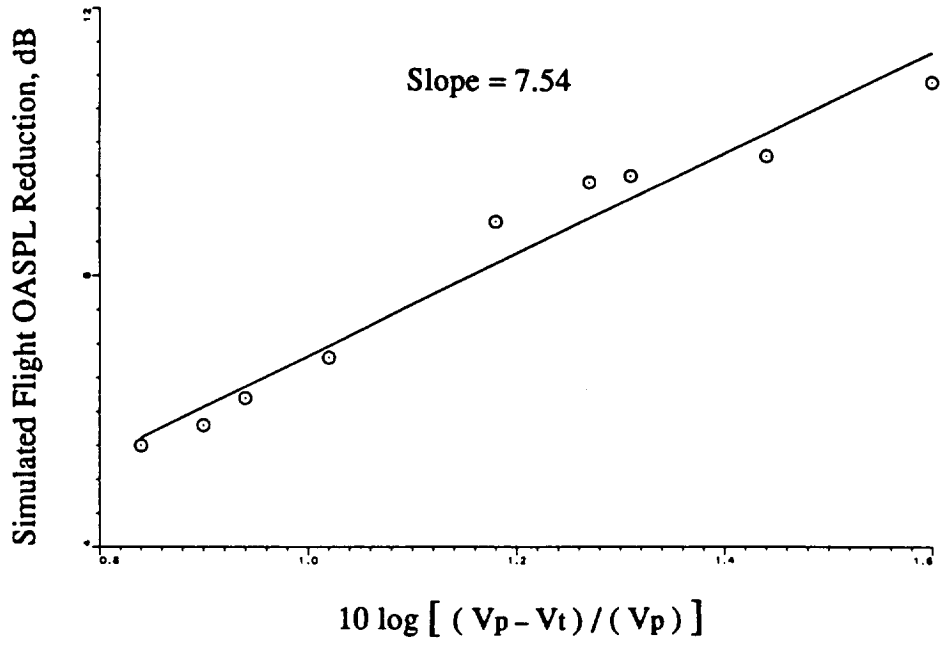

Figure 51. Correlations of Jet Noise OASPL Reductions with the Relative Jet Velocity Parameter for 135–degrees Angle

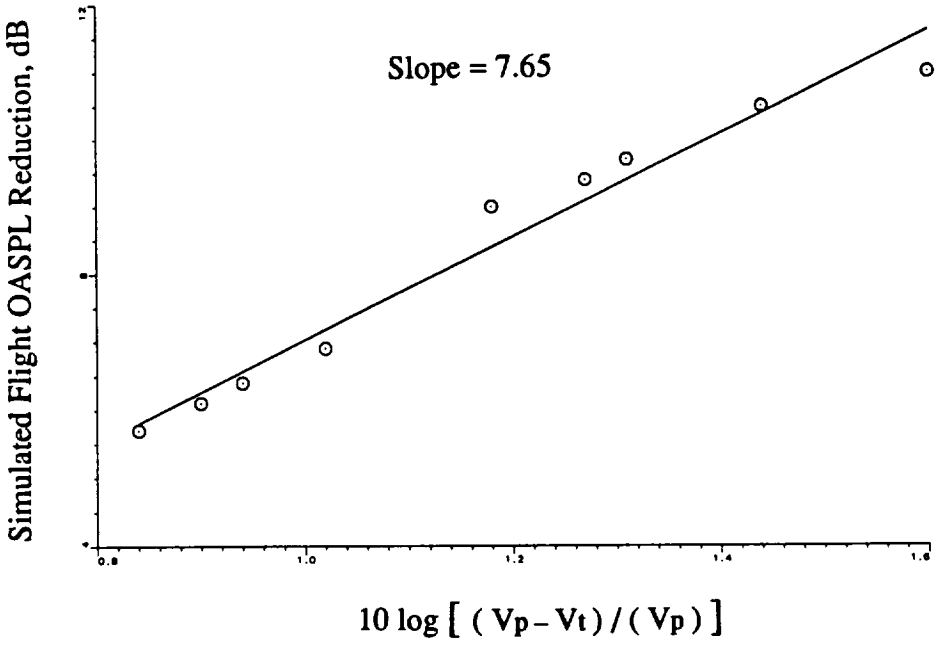

Figure 52. Correlations of Jet Noise OASPL Reductions with the Relative Jet Velocity Parameter for 140–degrees Angle

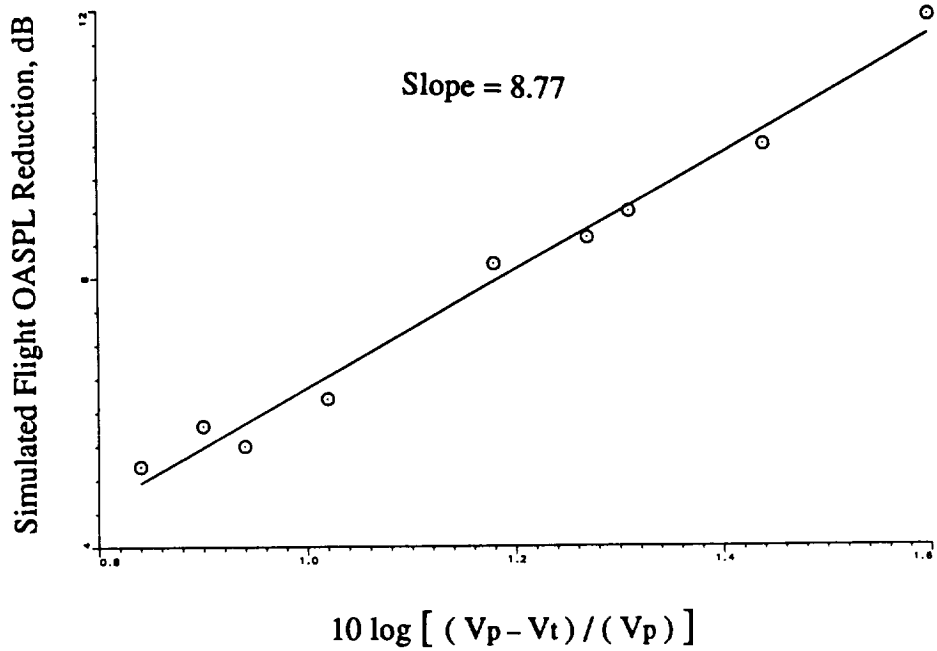

Figure 53. Correlations of Jet Noise OASPL Reductions with the Relative Jet Velocity Parameter for 145–degrees Angle

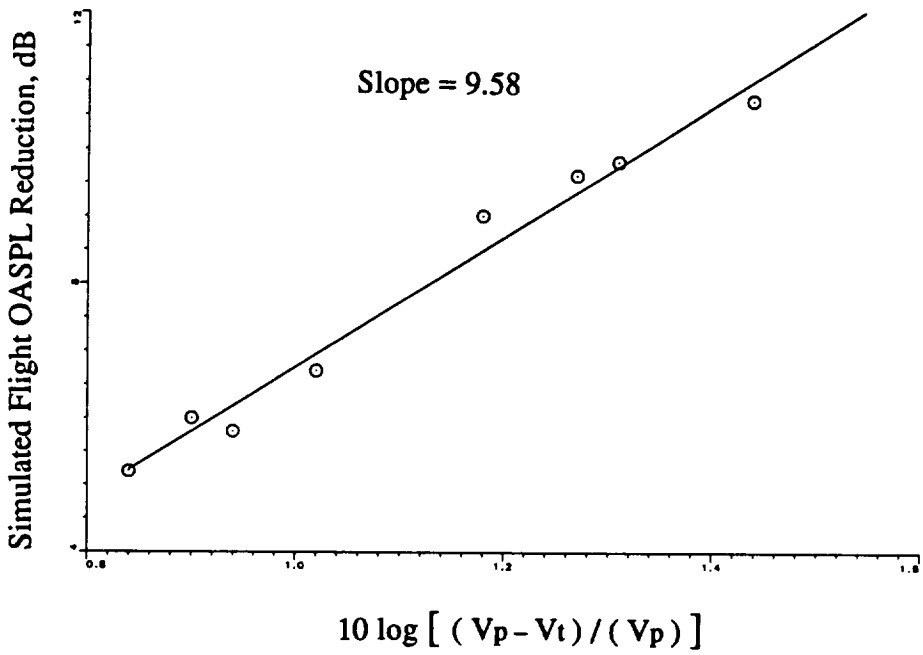

Figure 54. Correlations of Jet Noise OASPL Reductions with the Relative Jet Velocity Parameter for 150–degrees Angle

Table 3. UHBR Jet Noise Relative Velocity Exponents for Angles 80 through 150 degrees.

Angles	**Relative Velocity Exponents**	
(deg.)	ADP UHBR Jet	SAE (for Vp < 1.10 sonic speed)
80	5.58	0.4
90	5.17	1.0
100	5.57	1.9
110	5.83	3.0
120	7.55	4.7
130	8.24	7.0
135	7.54	8.5
140	7.65	10.2
145	8.77	10.3
150	9.58	10.4

6.0 SUMMARY OF ACOUSTIC RESULTS

Results showed that the jet noise from the 1/15–scaled ADP model nozzle can be successfully scaled to the ADP fullscale engine jet noise levels. The predicted levels of jet noise in the ADP engine were significantly lower than the levels predicted for fan and core noise. Fan and core noise dominated the ADP engine noise spectra at most angles for all power settings. Jet noise tended to dominate the low frequency portion of the engine noise spectra for angles greater than 140 degrees. The current SAE jet noise prediction methods do not adequately predict the jet noise levels from the ultra–high bypass ratio ADP type coaxial nozzle. This is because the current SAE methods were developed from model–scale nozzles and turbofan engine data with bypass ratios less than 6.5, and secondary to primary nozzle area ratios less than 3.5. By comparison, the bypass ratio of the ADP nozzle ranged from 10 to 12, and nozzle area ratio from 7.1 to 7.4. The SAE coaxial jet prediction overestimated the UHBR jet noise by 5 to 6 decibels across the low frequency portion of the spectra. A simple method of subtracting 6 dB from the predicted levels for the "merged and secondary flow" source components of the coaxial jet prediction may be the most expedient method of predicting the UHBR jet noise. These UHBR jet noise data will be an excellent addition to the SAE jet noise database, and could be used to revise and expand the current SAE Coaxial Jet Noise Prediction for bypass ratios greater than 6.5. The simulated jet noise flight effects with tunnel Mach numbers up to 0.35 yielded some excellent results. The reductions in jet noise levels were across the entire jet noise spectra, suggesting that the flight effects affected all source components in the coaxial jet, unlike the flight effects for "mixer–type" nozzles where only the low–frequency portions of the static jet noise spectra are affected. The relative velocity exponents for the UHBR jet noise flight effects ranged from 5.17 for 90 degrees to 9.58 for 150 degrees angle. These values, significantly higher than those for the SAE lower bypass turbofan coaxial jets for angles up to 130 degrees, are currently the only set of test data on relative velocity exponents for the UHBR jet noise. Since the UHBR jet noise is not considered to be the dominant low–frequency noise source for the ADP engine at static condition, it is even less of a problem at flight because of the relatively large noise reduction with flight.

7.0 REFERENCES

1. Amiet, R.K., "Correction of Open Jet Wind Tunnel Measurements for Shear Layer Refraction," AIAA Paper 75–532, 1975.

2. Kozlowski, H., Packman, A. B., "Flight Effects on the Aerodynamic and Acoustic Characteristics of Inverted Profile Coannular Nozzles," NASA CR–3018, August 1978.

3. Bass, W.E., Shields, F.D., "Atmospheric Absorption of High Frequency Noise and Application to Fractional Octave Bands", University of Mississippi, NASA CR–2760, June 1977.

4. Proposed Coaxial Jet Noise Prediction Procedure, (M.J.T. Smith to the Society of Automotive Engineers: Aerospace Recommended Practice, ARP 876 Revision C), November 1975.

REPORT DOCUMENTATION PAGE

Form Approved
OMB No. 0704-0188

1. AGENCY USE ONLY (*Leave blank*)	2. REPORT DATE	3. REPORT TYPE AND DATES COVERED
	October 1994	Final Contractor Report

4. TITLE AND SUBTITLE

Ultra-High Bypass Ratio Jet Noise

5. FUNDING NUMBERS

WU-538-03-11
C-NAS3-26618

6. AUTHOR(S)

John K.C. Low

7. PERFORMING ORGANIZATION NAME(S) AND ADDRESS(ES)

United Technology Corporation
Pratt & Whitney Division
East Hartford, Connecticut

8. PERFORMING ORGANIZATION REPORT NUMBER

E-9172

9. SPONSORING/MONITORING AGENCY NAME(S) AND ADDRESS(ES)

National Aeronautics and Space Administration
Lewis Research Center
Cleveland, Ohio 44135-3191

10. SPONSORING/MONITORING AGENCY REPORT NUMBER

NASA CR-195394

11. SUPPLEMENTARY NOTES

Project Manager, Eugene A. Krejsa, Propulsion Systems Division, NASA Lewis Research Center, organization code 2770, (216) 433-3951.

12a. DISTRIBUTION/AVAILABILITY STATEMENT

Unclassified - Unlimited
Subject Category 71

12b. DISTRIBUTION CODE

13. ABSTRACT (*Maximum 200 words*)

The jet noise from a 1/15 scale model of Pratt and Whitney Advanced Ducted Propulsor (ADP) were measured in the United Technology Research Center anechoic research tunnel (ART) under a range of operating conditions. Conditions were chosen to match engine operating conditions. Data were obtained at static conditions and at wind tunnel Mach numbers of 0.2, 0.27, and 0.35 to simulate inflight effects on jet noise. Due to a temperature dependence of the secondary nozzle area, the model nozzle secondary to primary area ratio varied from 7.12 at 100% thrust to 7.39 at 30% thrust. The bypass ratio varied from 10.2 to 11.8 respectively. Comparison of the data with predictions using the current Society of Automotive Engineers (SAE) Jet Noise Prediction Method showed that the current prediction method overpredicted the ADP jet noise by 6 decibels. The data suggest that a simple method of subtracting 6 decibels from the SAE Coaxial Jet Noise Prediction for the merged and secondary flow source components would result in good agreement between predicted and measured levels. The simulated jet noise flight effects with wind tunnel Mach numbers up to 0.35 produced jet noise inflight noise reductions up to 12 decibels. The reductions in jet noise levels were across the entire jet noise spectra, suggesting that the inflight effects affected all source noise source components.

14. SUBJECT TERMS

Acoustics; Jet noise

15. NUMBER OF PAGES

16. PRICE CODE

17. SECURITY CLASSIFICATION OF REPORT	18. SECURITY CLASSIFICATION OF THIS PAGE	19. SECURITY CLASSIFICATION OF ABSTRACT	20. LIMITATION OF ABSTRACT
Unclassified	Unclassified	Unclassified	